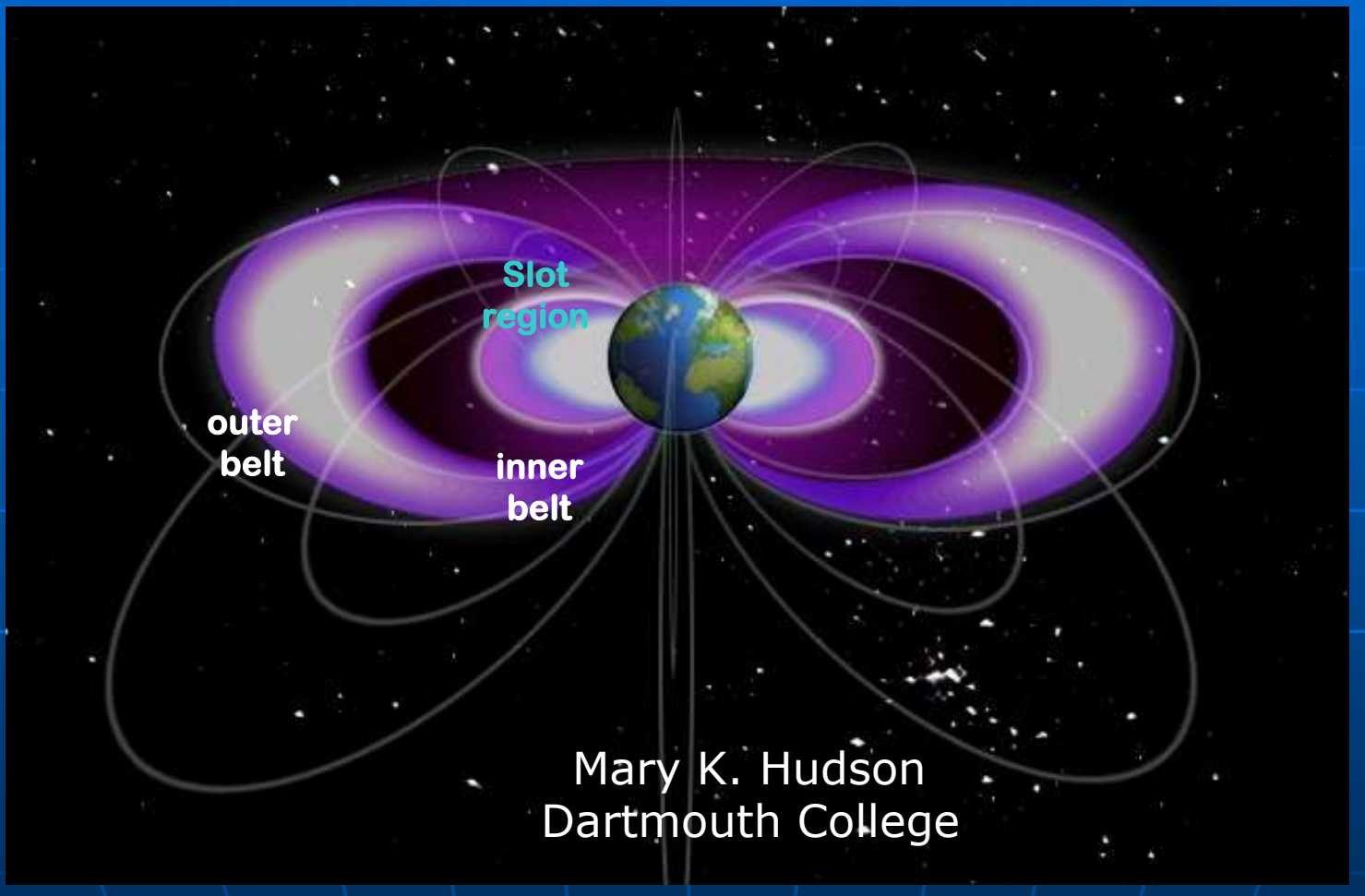
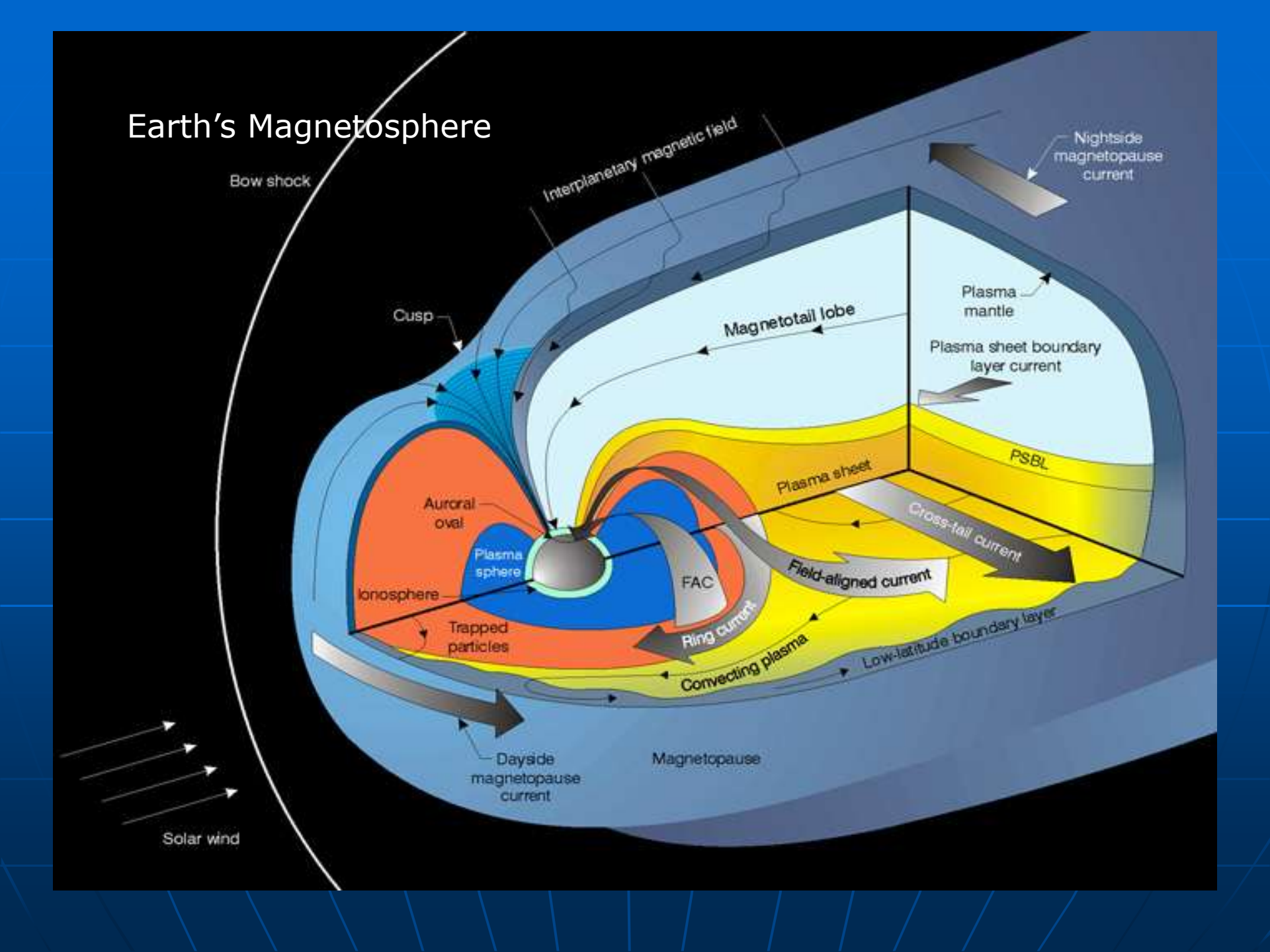
#### Plasma Processes in the Magnetosphere: Radiation Belt Response to Solar Wind Drivers

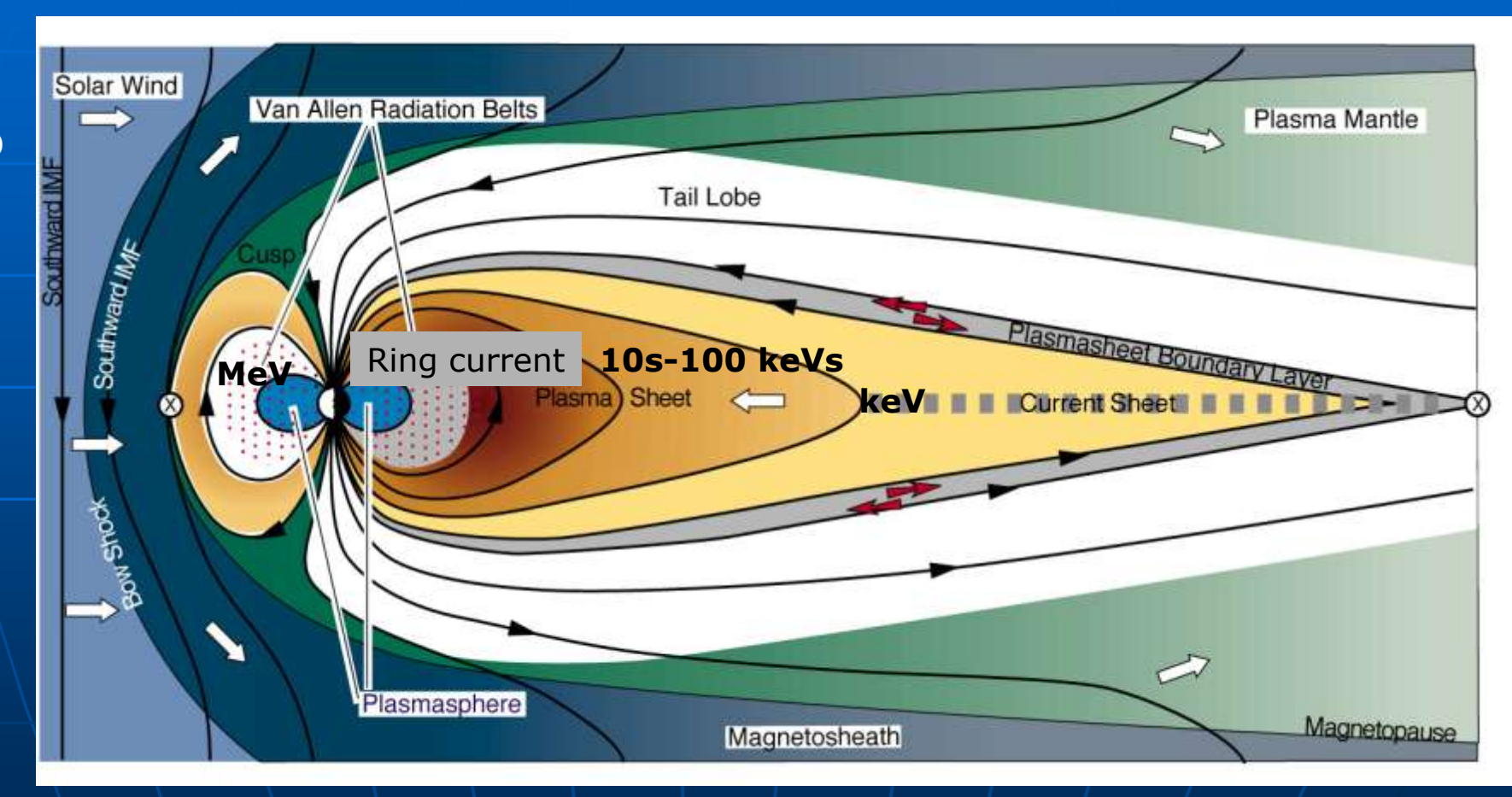


Contributions: T. Brito, Zhao Li, S. Elkington, B. Kress



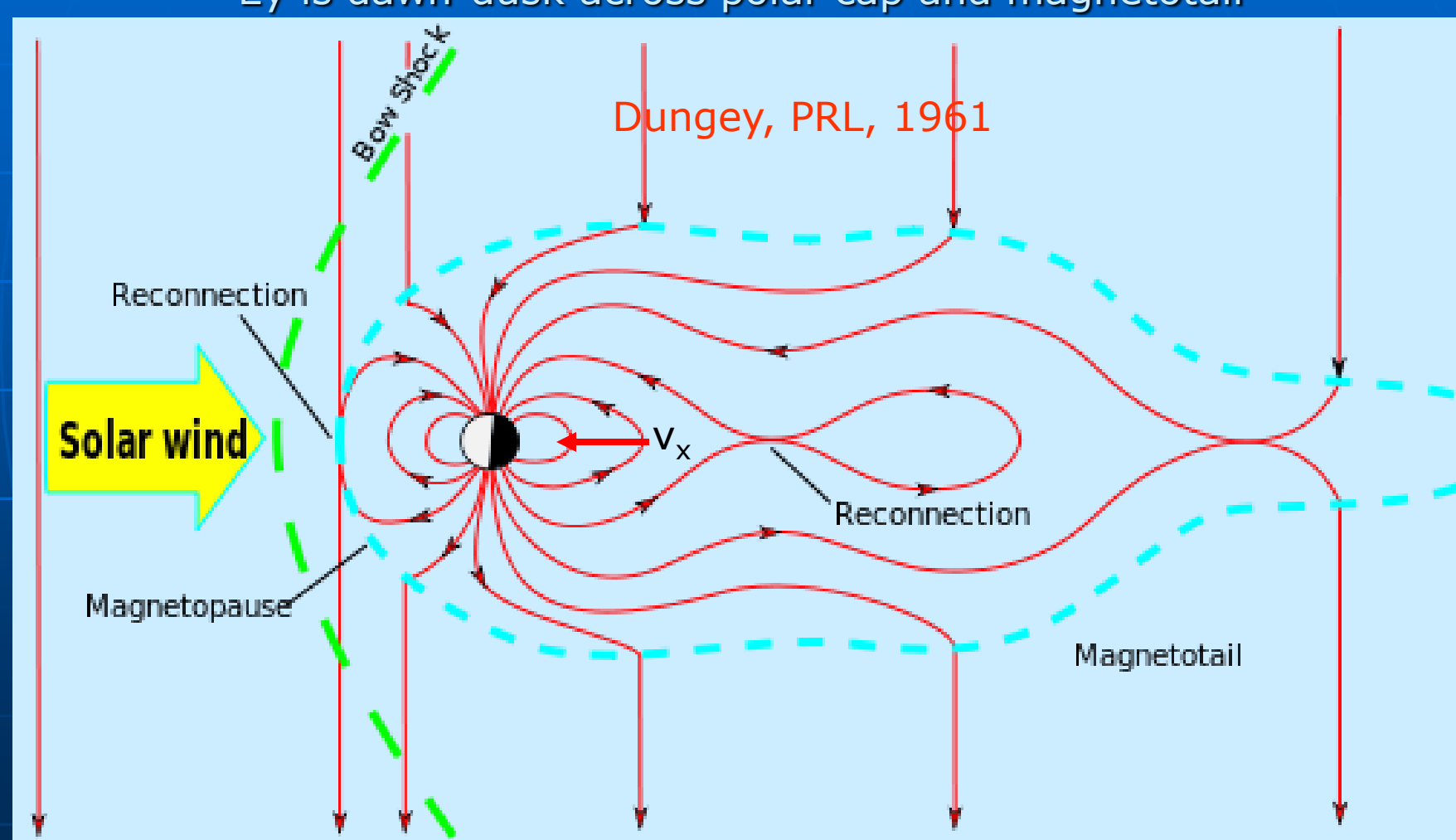
### Magnetosphere Overview

eV el keV p



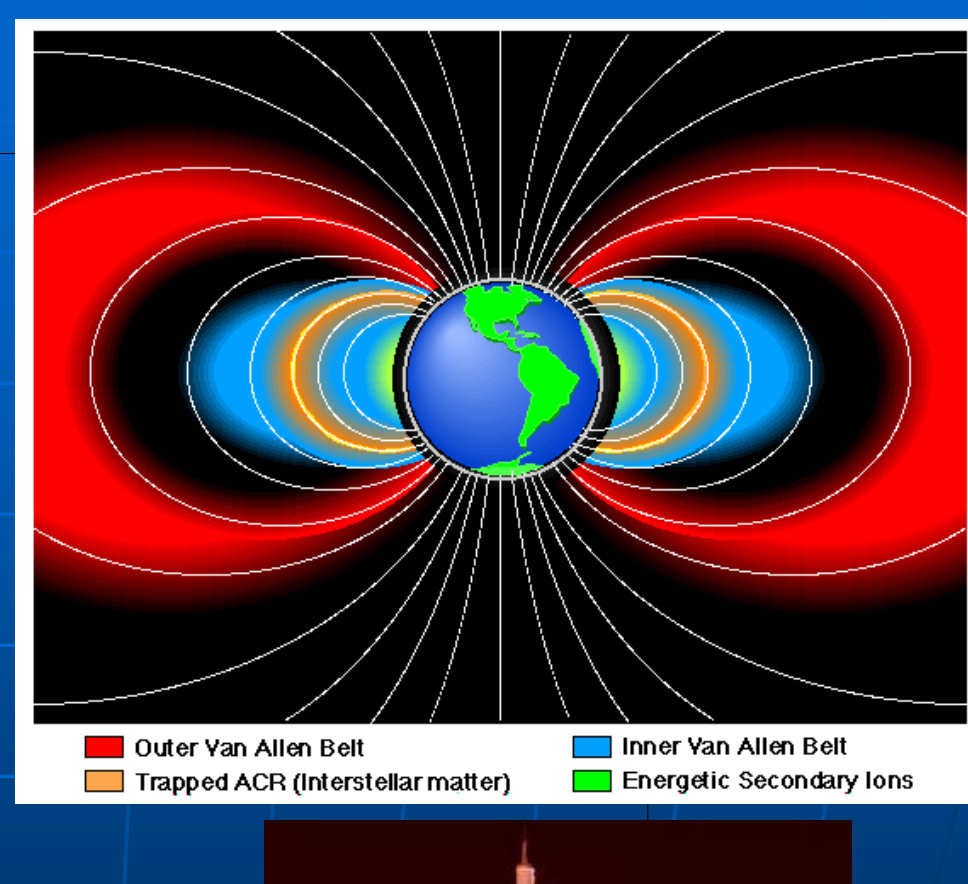
# Mag Convection: $E_{y=} - v_x \times B_z$

Ey is dawn-dusk across polar cap and magnetotail



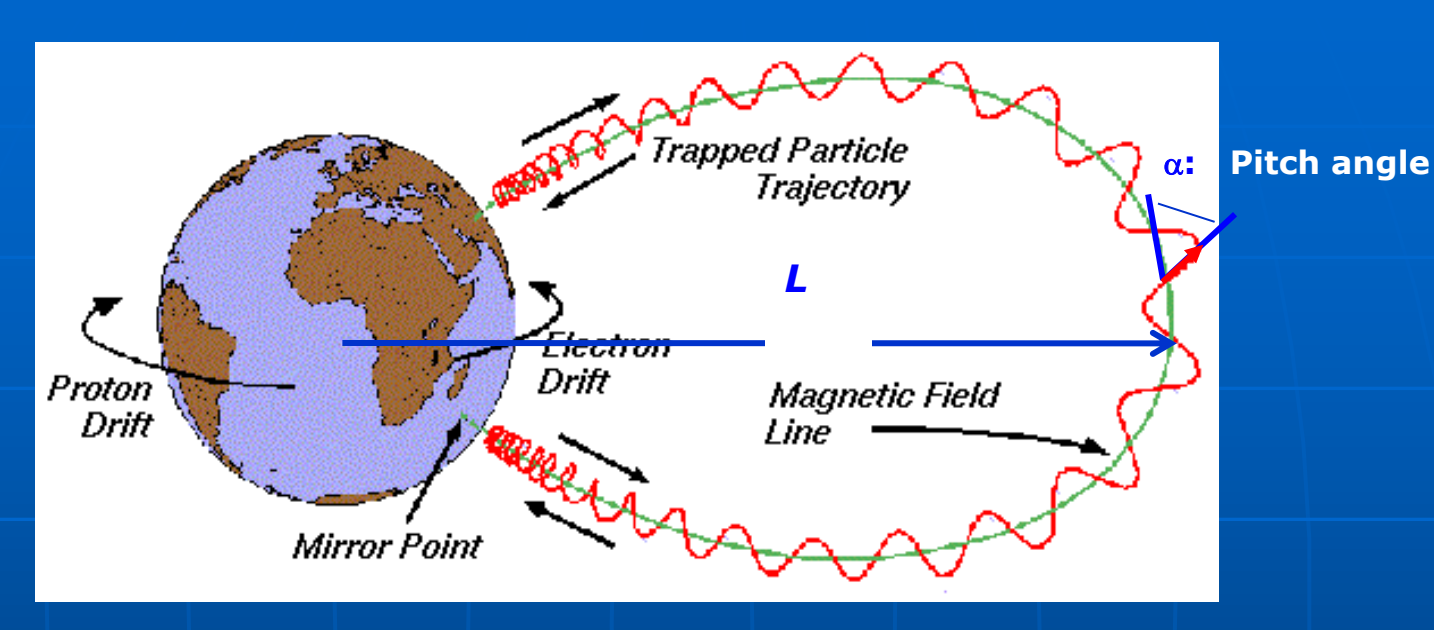
### Radiation Belts: The Big Picture

- The Radiation Belts consist of energetic charged particles (plasma) trapped by Earth's magnetic field
- Historic discovery in 1958 by the Explorer I under Dr. James Van Allen at the University of Iowa.
- The trapped radiation was first mapped out by Sputnik 3, Explorer IV, Pioneer III and Luna 1.
- Energetic electrons form two distinct radiation belts, while protons form a single belt.





#### **Adiabatic invariants**



#### **Adiabatic invariants:**

- Cyclotron motion:

$$\mu = \frac{p_{\perp}^2}{2mB} = \frac{p^2 \sin^2 \alpha}{2mB}$$

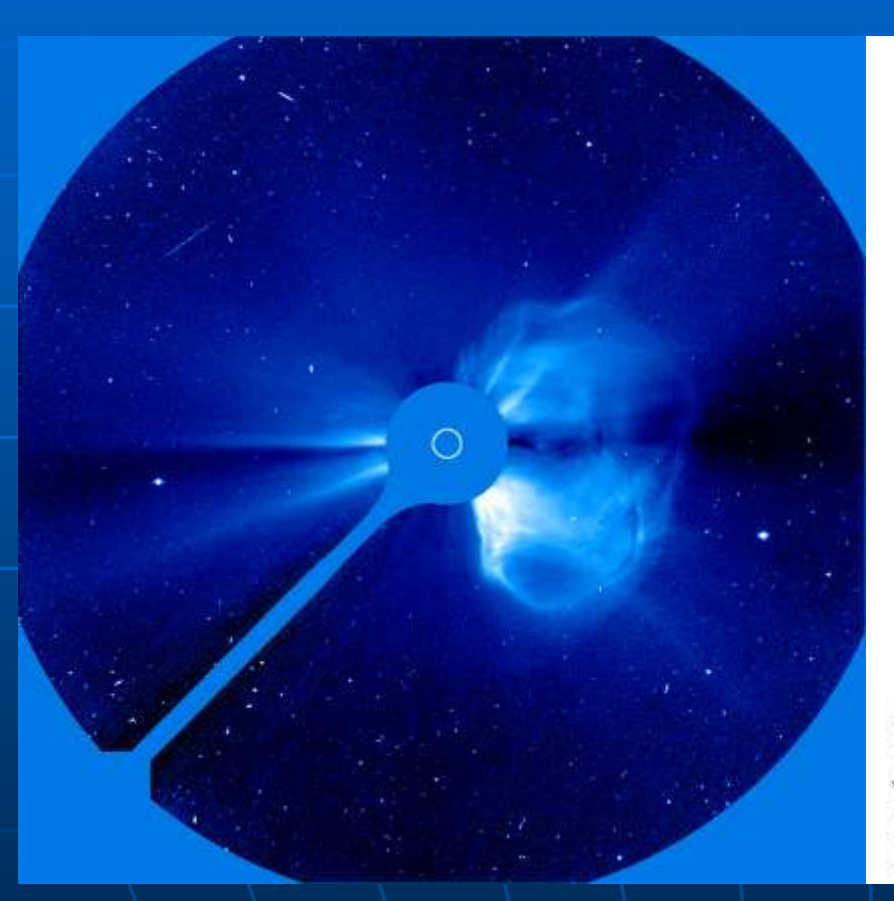
[MeV/G]

– Bounce motion:

$$K = \int_{s_m}^{s_{m'}} \left[ B_m - B(s) \right] ds$$

$$\Phi = \iint_{S_0} \mathbf{da} \cdot \mathbf{B}$$
 and  $L^* = \frac{2\pi M}{\Phi R_E}$ 

# CME vs. High Speed Stream Source of MeV Electron Events



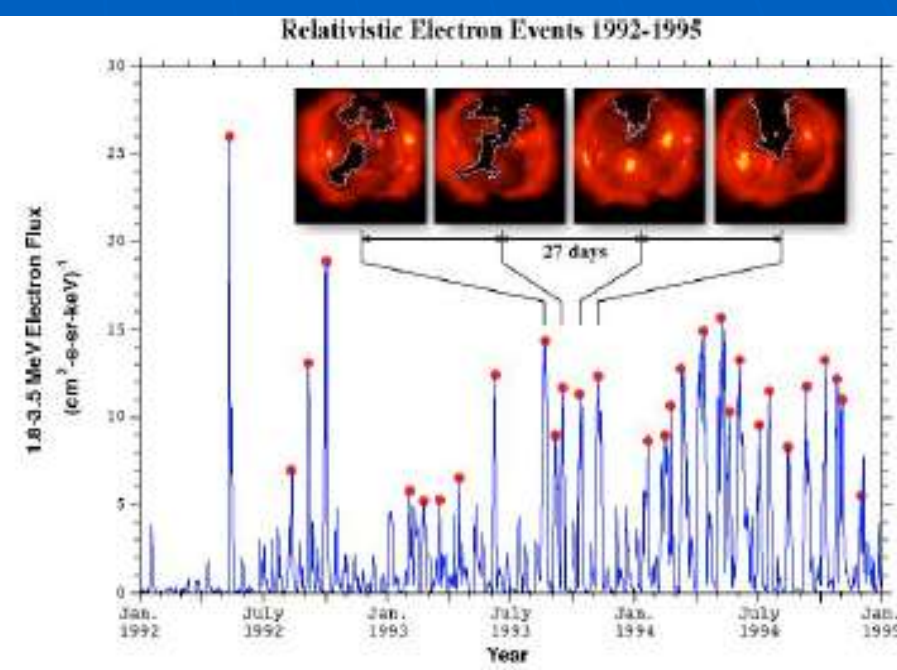
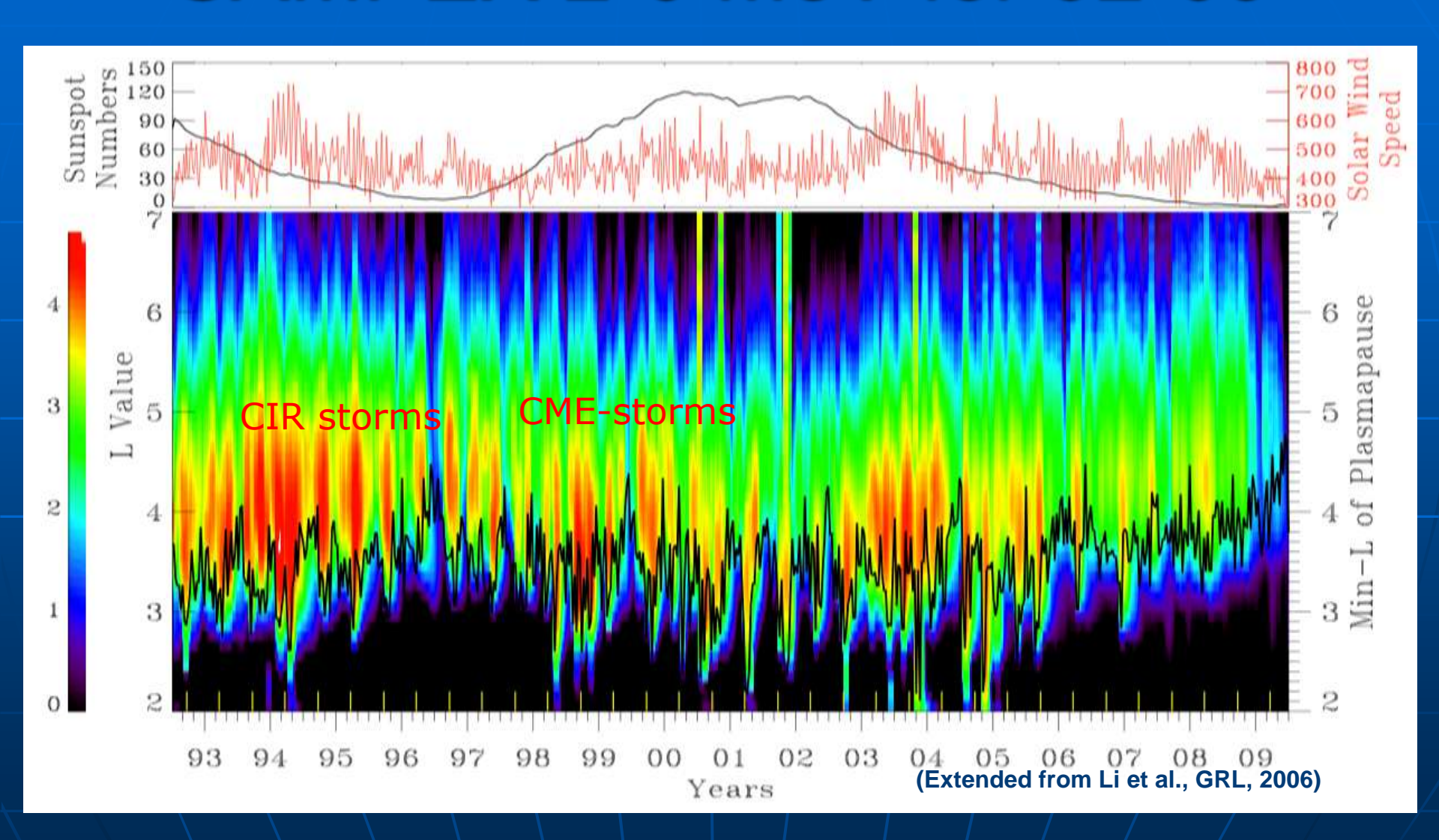
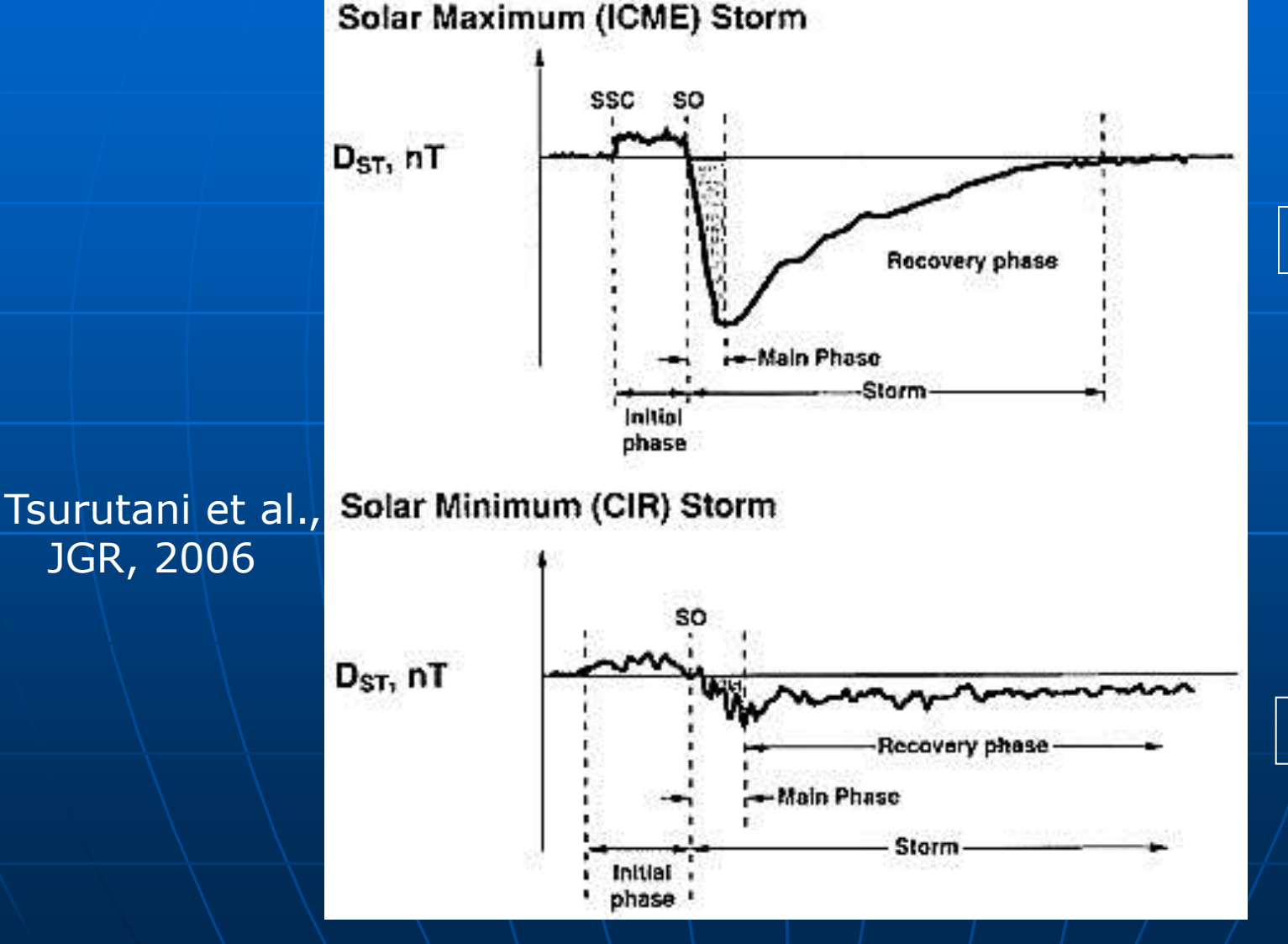


Figure 1. Daily average geosynchronous electron fluxes 1992-1995 showing quasi-periodic response to high speed solar wind streams from coronal holes. [Reeves, 1998]

### SAMPEX 2-6 MeV for 92-09



### CME vs. CIR Storms

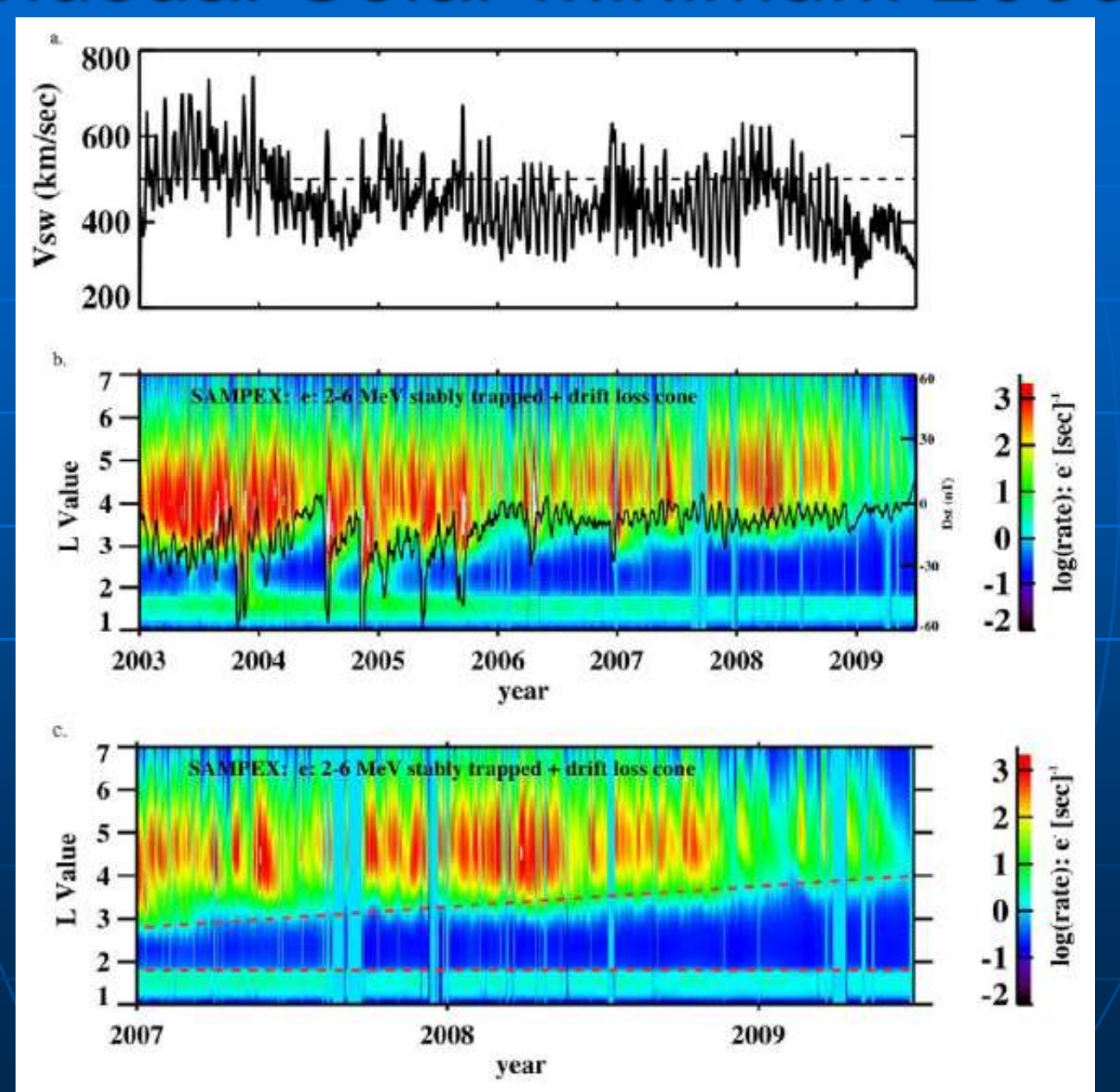


JGR, 2006

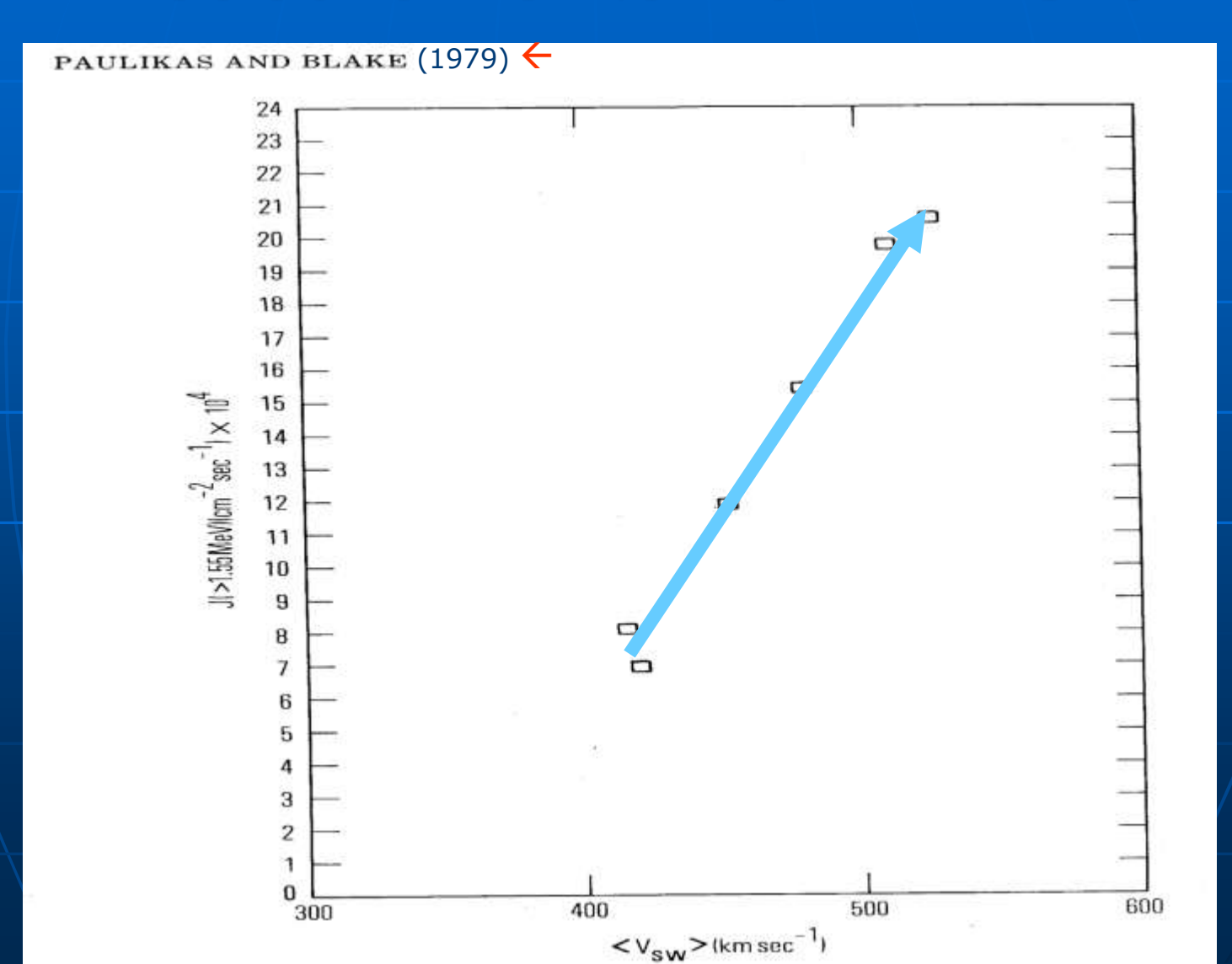
2 – 5 days

3.5 - 9 days

### **Unusual Solar Minimum 2009**



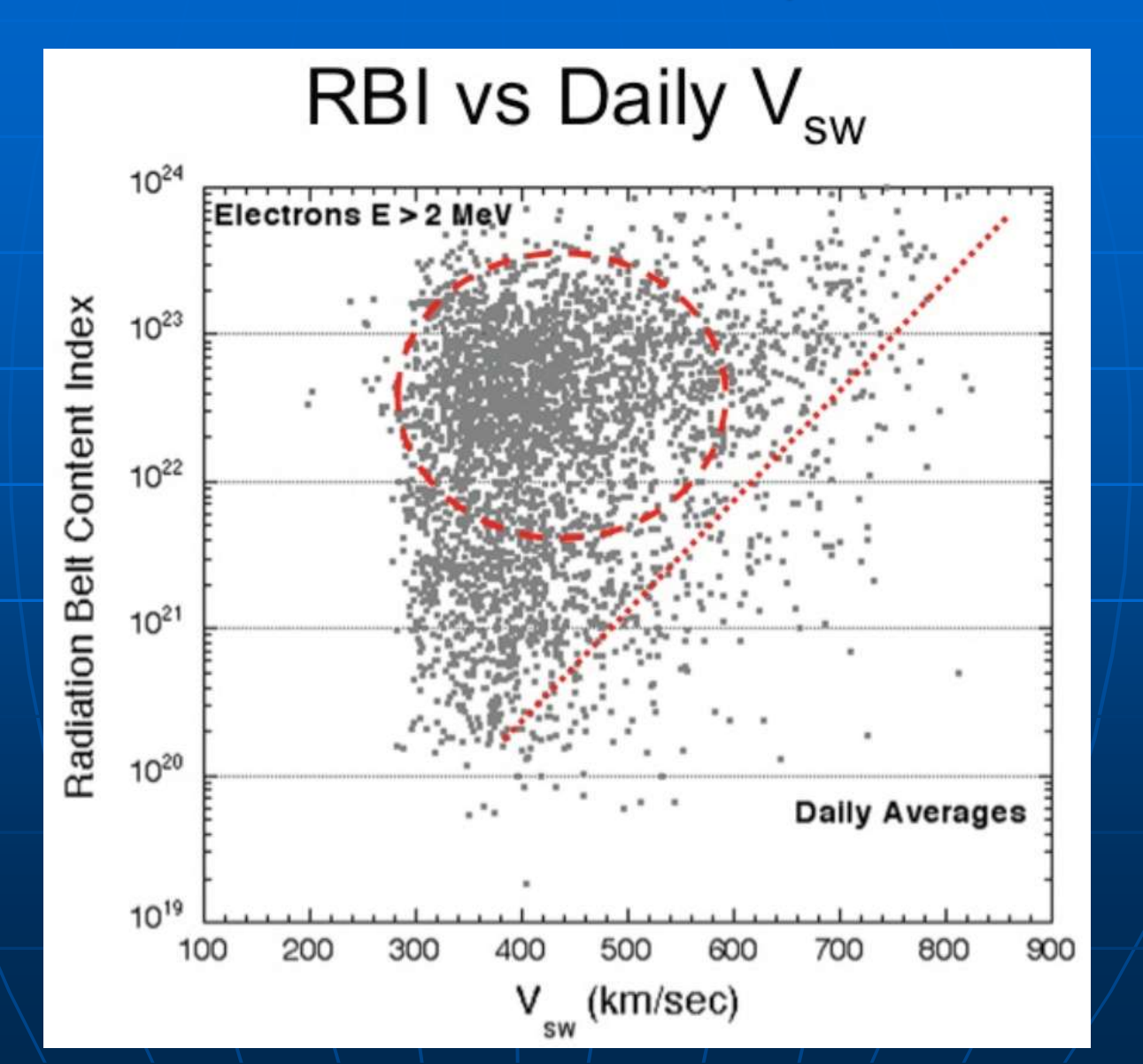
# Geosynchronous Electrons vs. v<sub>sw</sub> measurements from ATS-6



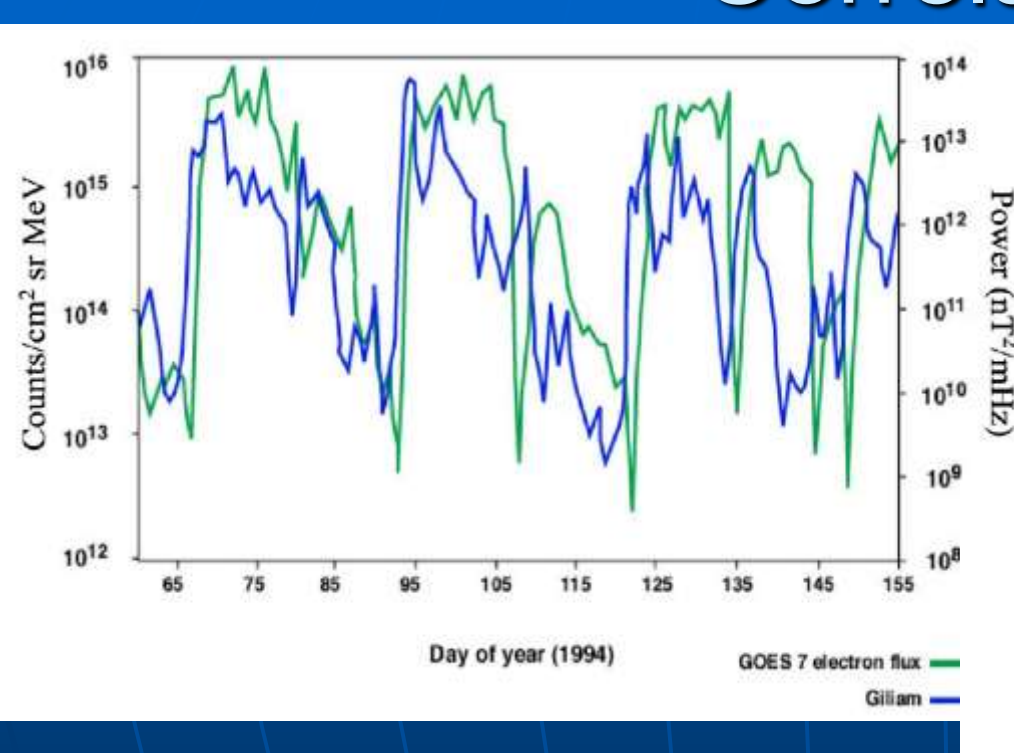
### SAMPEX Flux > 2 MeV, 2.5<L<6.5

Remains enhanced post-forcing

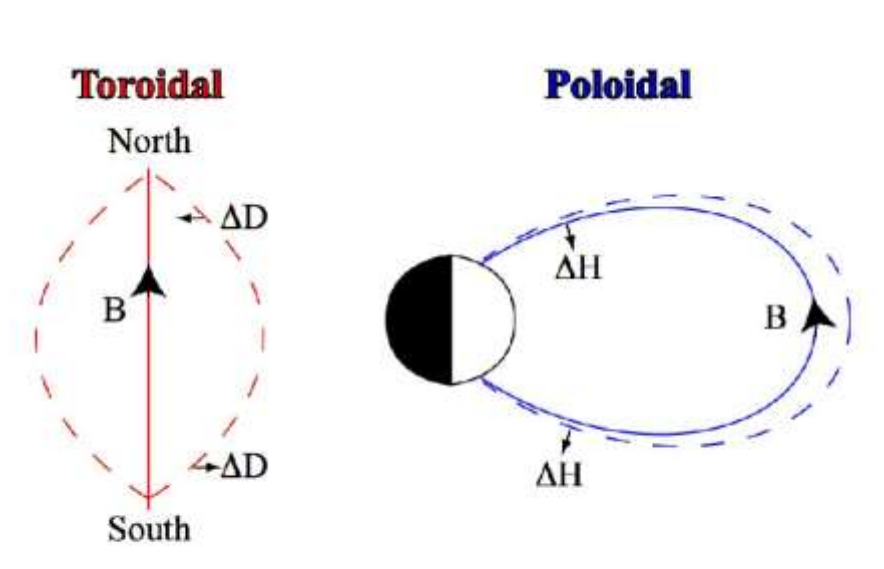
Baker et al., Space Weather, 2004



# ULF Wave-Relativistic Electron Correlation

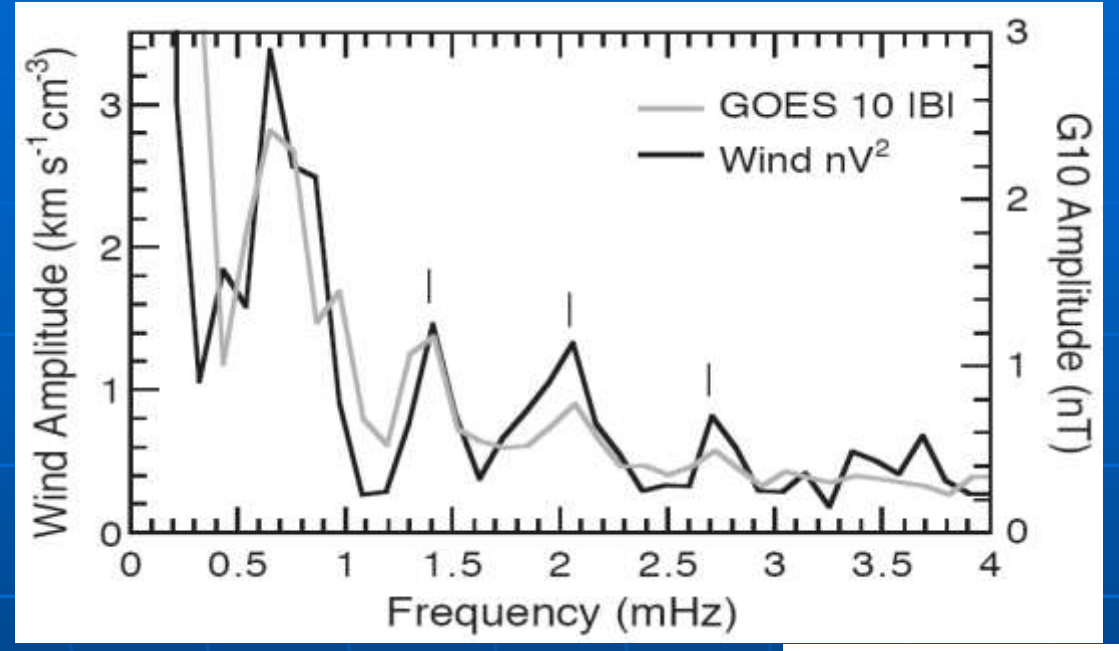


Rostoker et al., GRL, 1998



Fundamental Mode

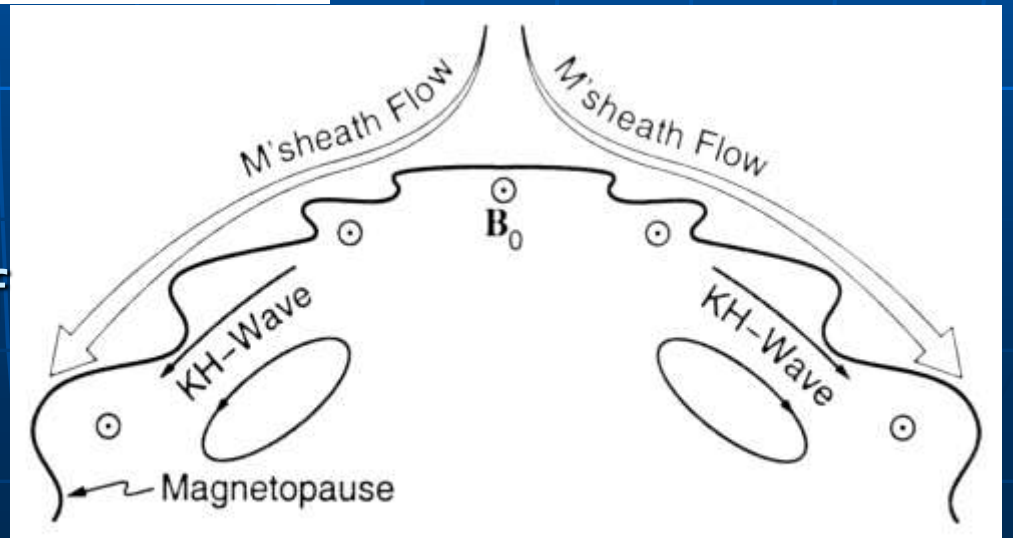
### Direct Coupling of Solar Wind ULF Waves



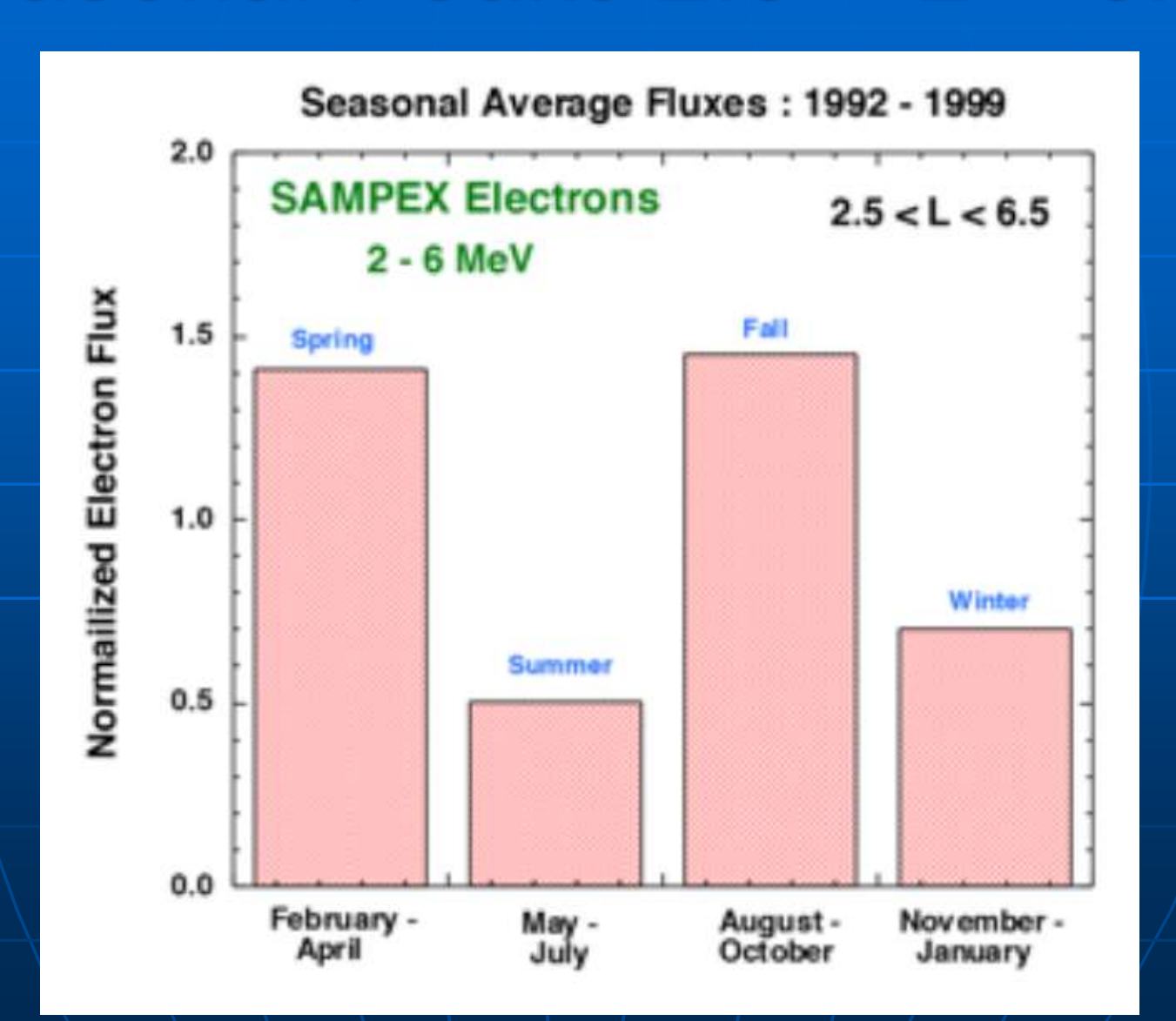
Kepko & Spence, JGR, 2003

Both correlated with Vsw

Or Convective Growth of Magnetopause K-H Waves Miura, JGR, 1992 Claudepierre et al., 2008

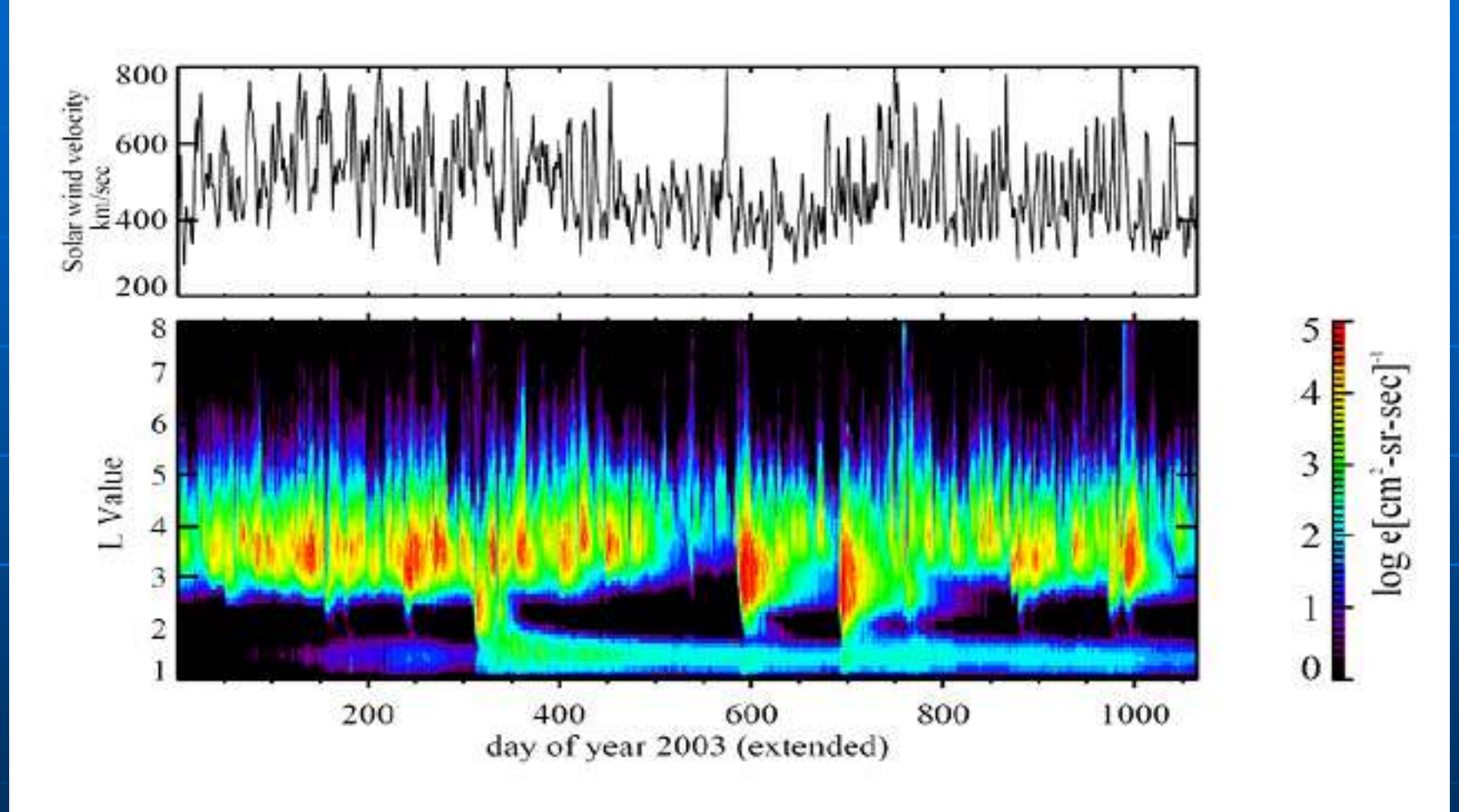


### Seasonal Peaks 2.5 < L < 6.5



Baker et al., GRL, 1999

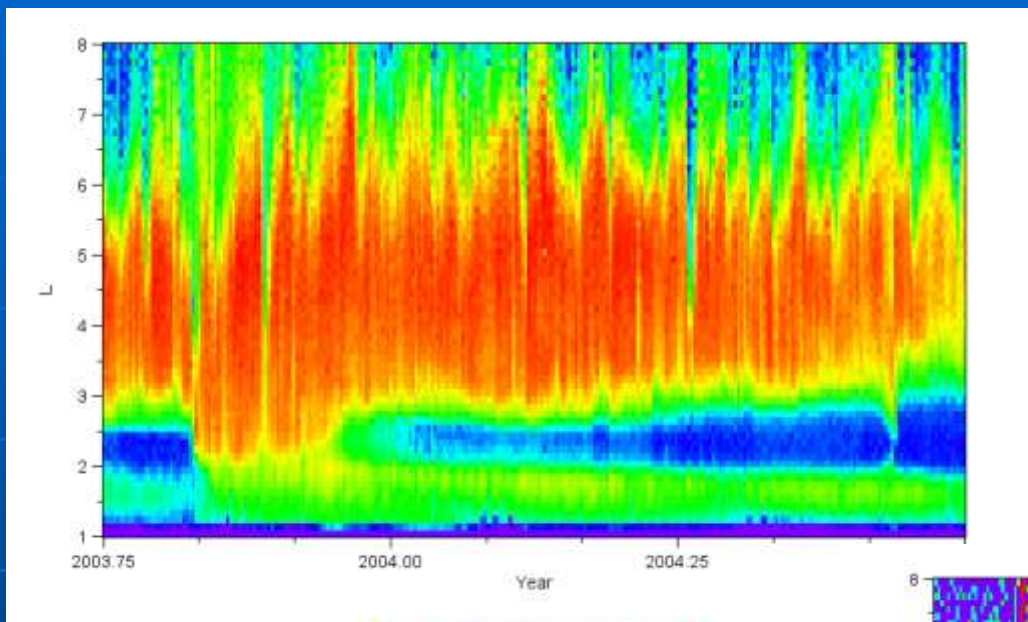
### SAMPEX 2-6 MeV for 03-05



ig. 5. (a) Solar wind speed and (b) energetic electron fluxes for the period 2003 through 2005. he format of the data is closely analogous to that in Fig. 3.

Baker et al., 2008

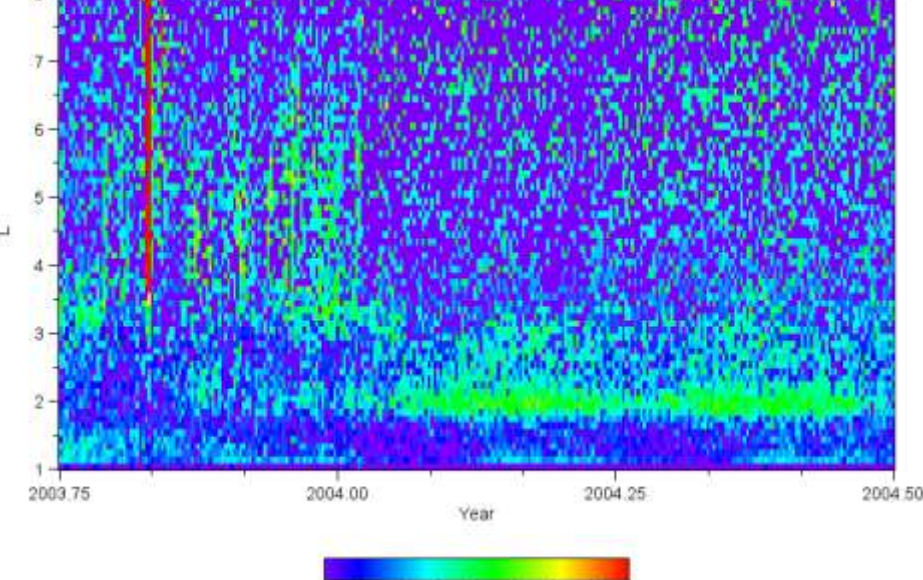
#### Halloween '03 2-6 and >10 MeV Electrons



-0.5 0.0

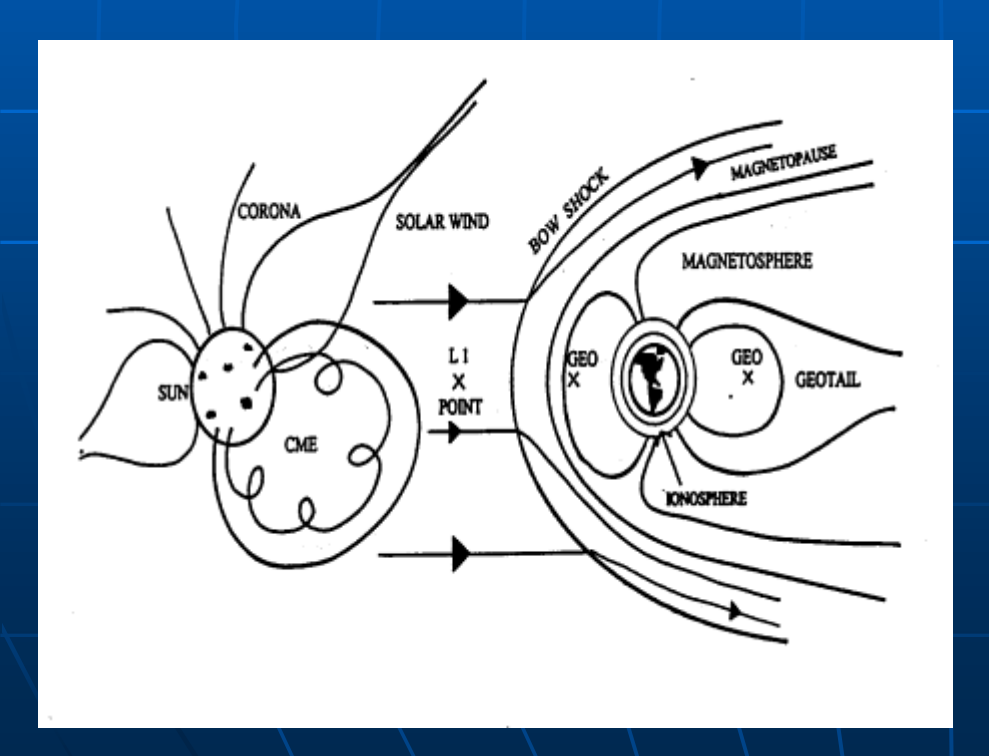
See filling of slot region on storm timescale (days) at 2-6 MeV (Baker et al., 2004)

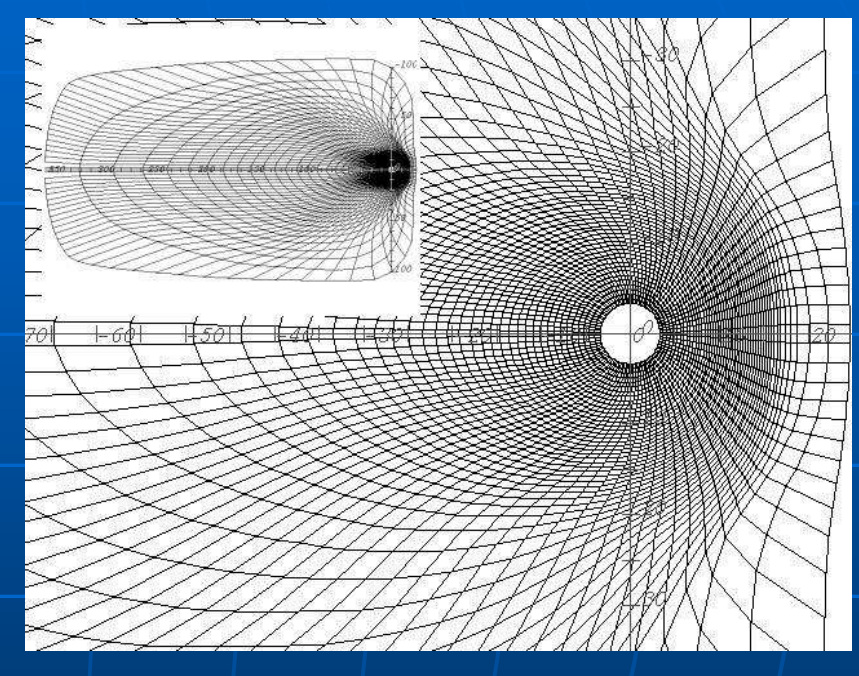
SAMPEX observes > 2 month delay in high > 10 MeV fluxes at low altitude (longer loss time



# Global MHD Simulations of Magnetosphere

Observations of the solar wind conditions made by satellites, operating at the L1 point where sun's = earth's gravity->input





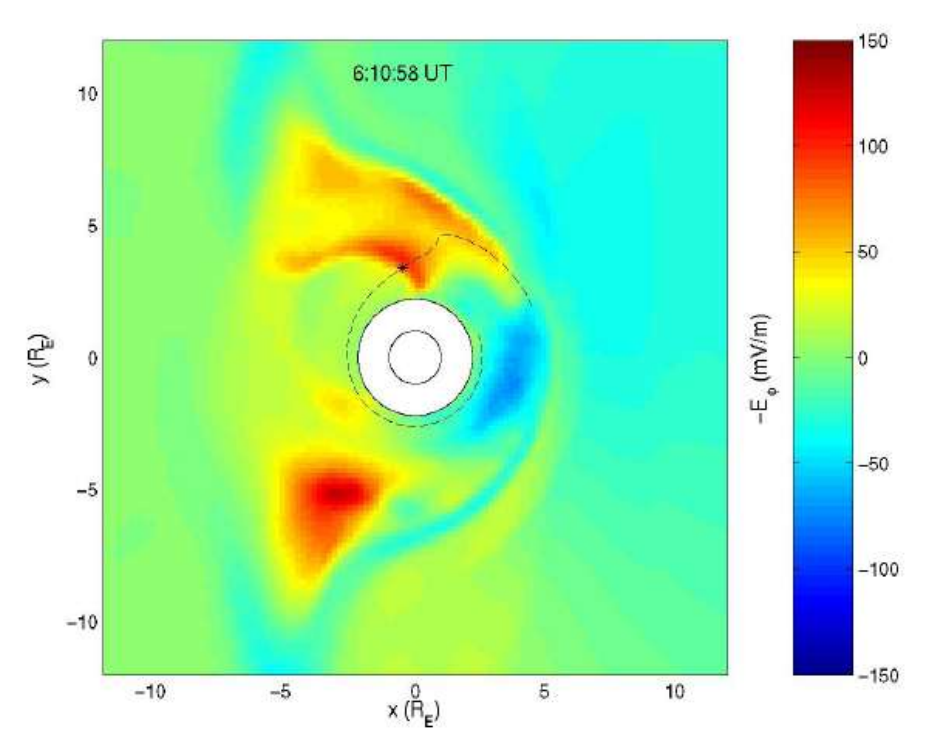
The ideal MHD equations are solved on a grid to simulate the response of the magnetosphere to the dynamic solar wind

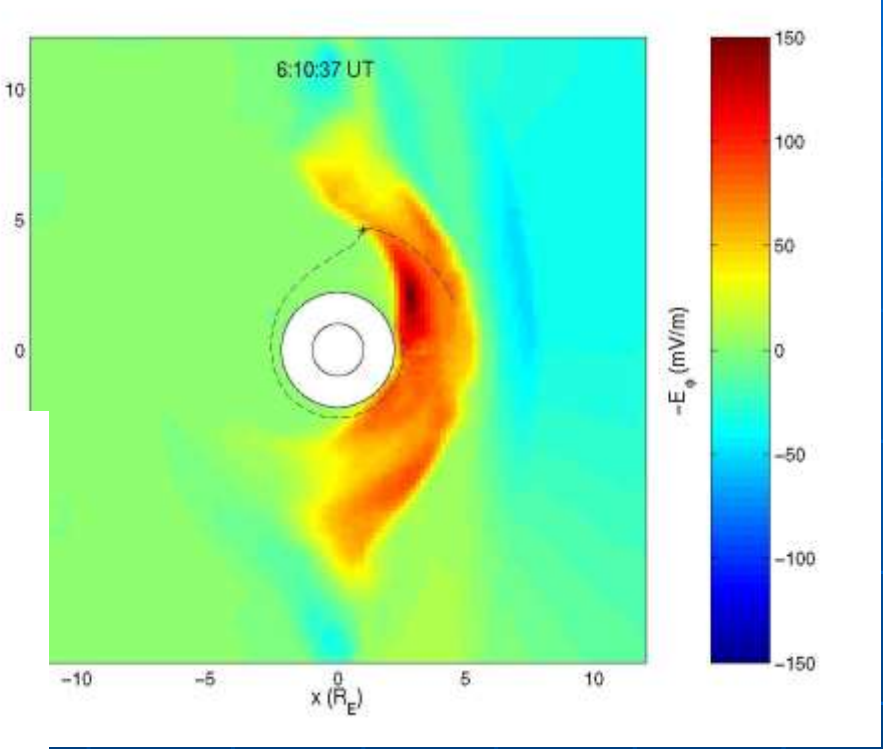
### Halloween '03 Shock Injection

MHD-test particle simulation LFM MHD code

W ~ 5 MeV → 15 MeV

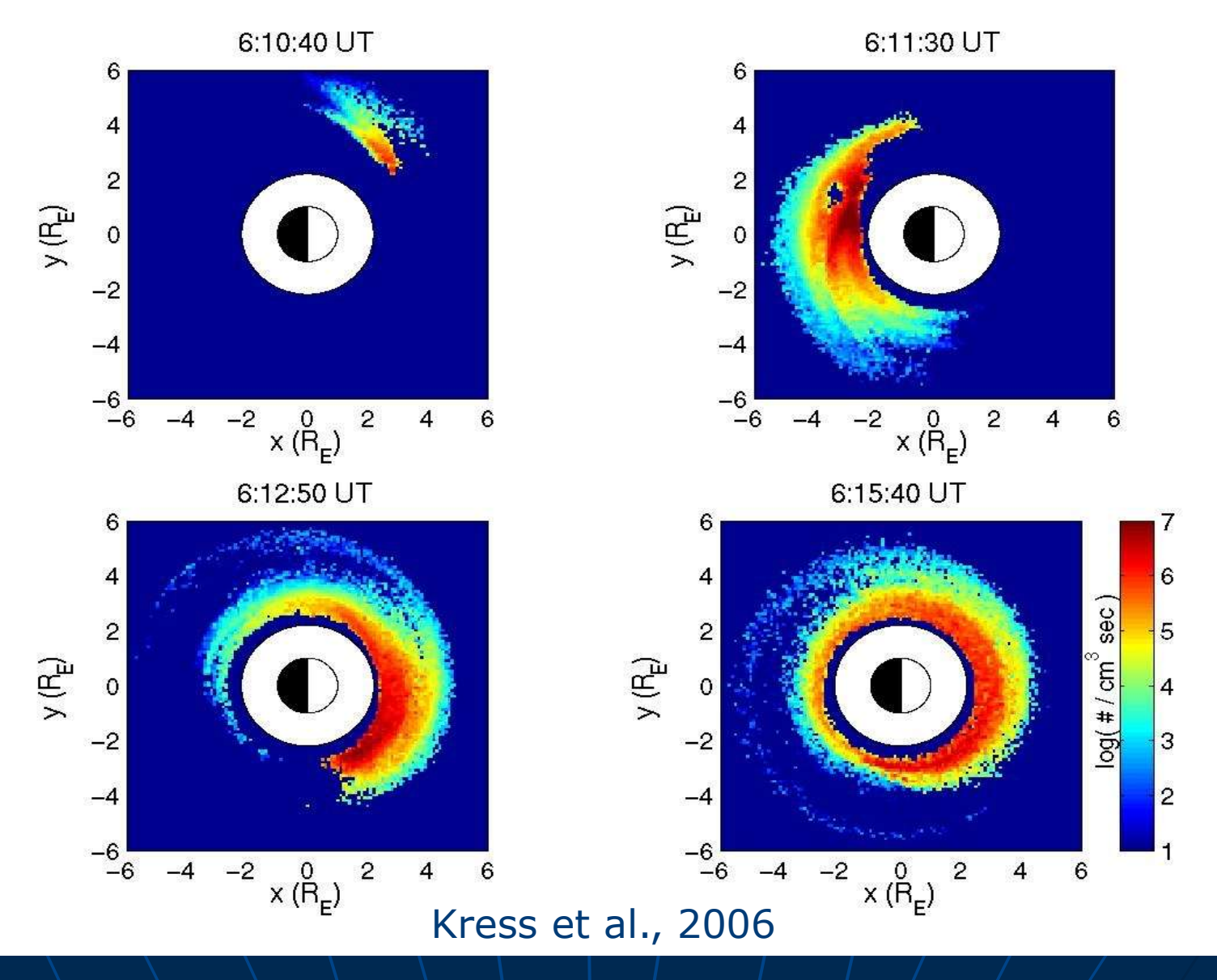
R  $\sim$  6 RE  $\rightarrow$  2.5 RE



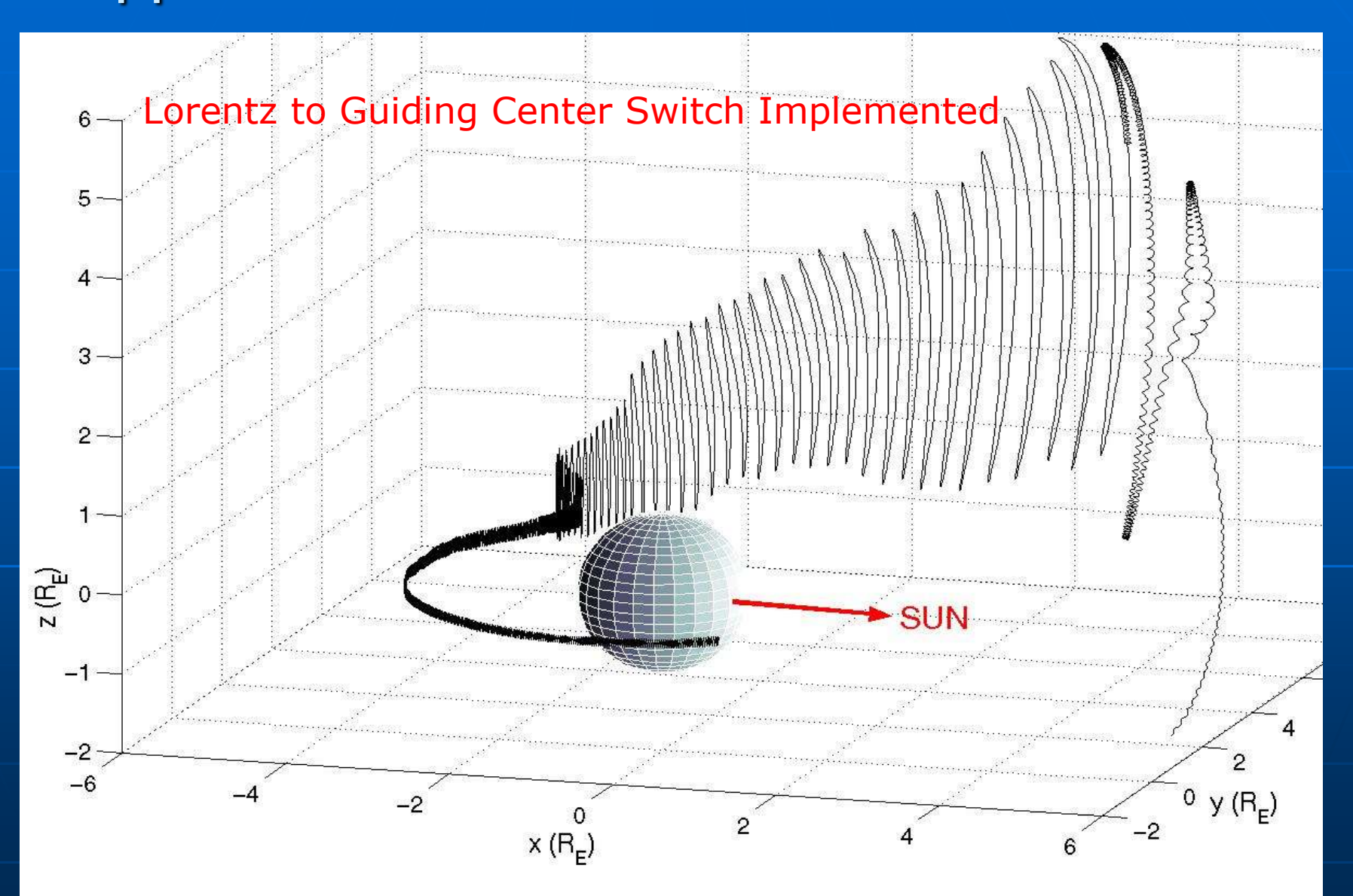


curl**E** = -dB/dt:  $dB_z/dt \rightarrow E_{phi}$ 29 October 2003 Kress et al., JGR, 07

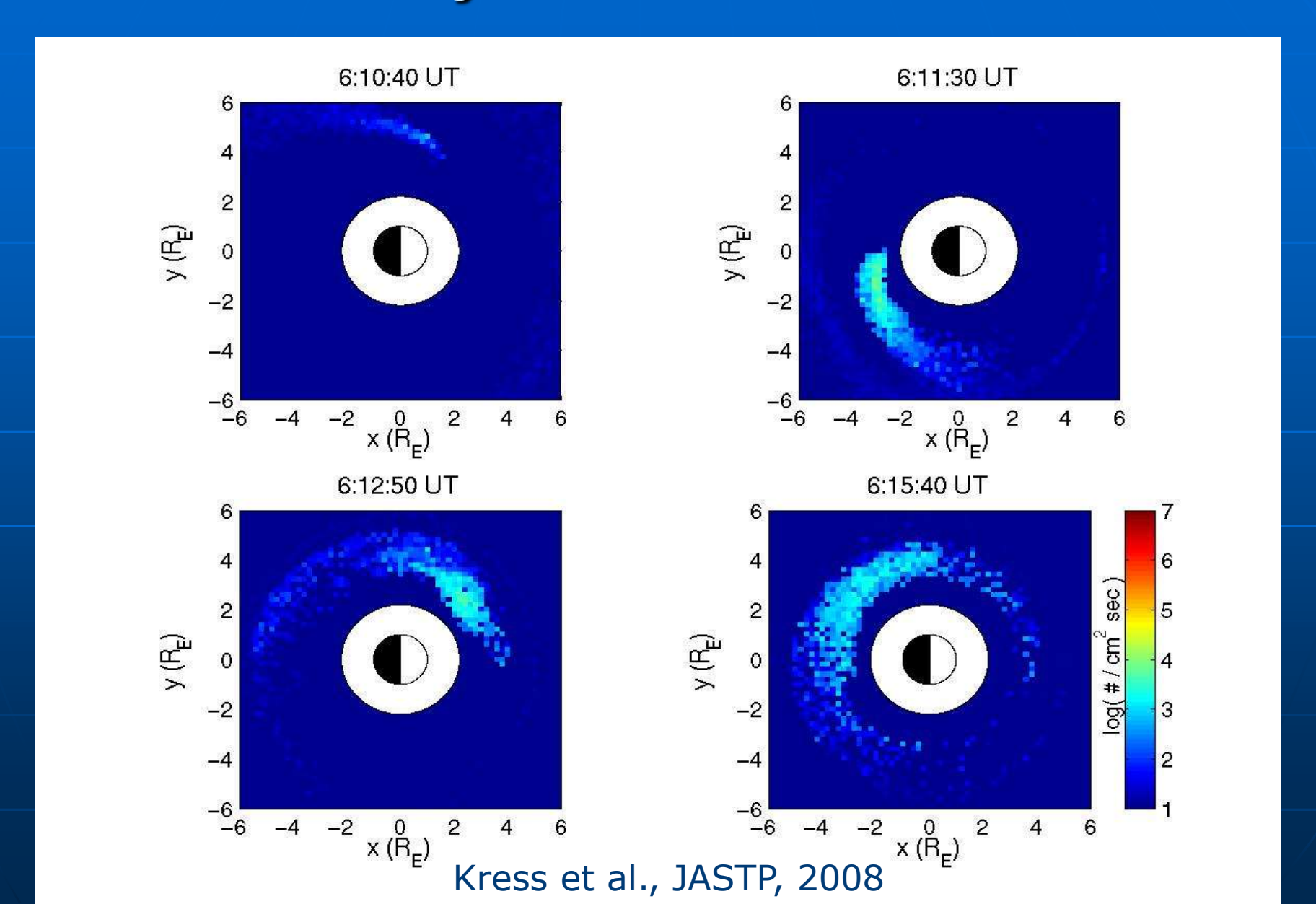
# Halloween '03 Shock Injection of >10 MeV (W0=1-7 MeV) Electrons



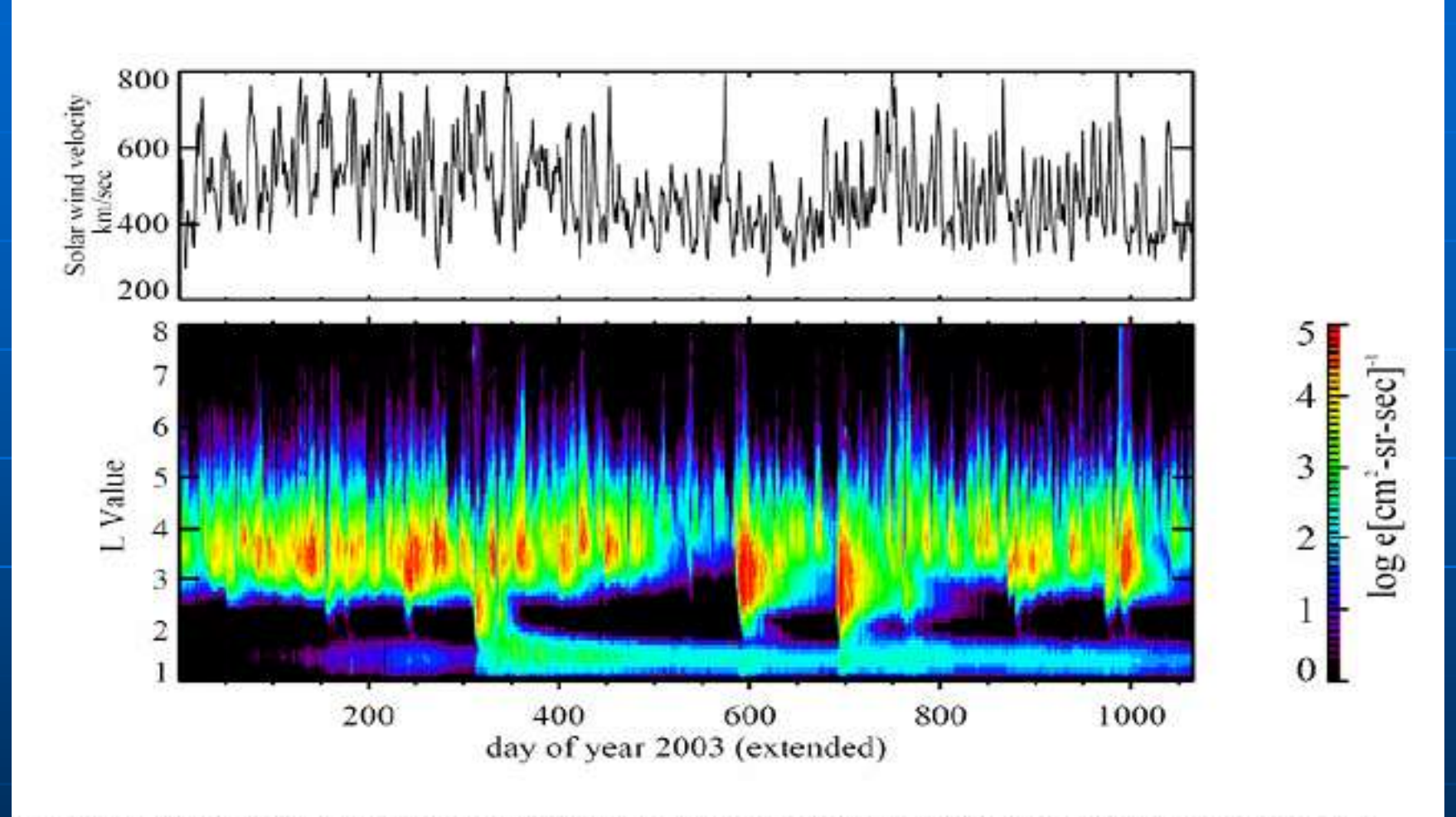
#### Trapped MeV electron in H-storm MHD fields



### H'storm Injection & SEE Source



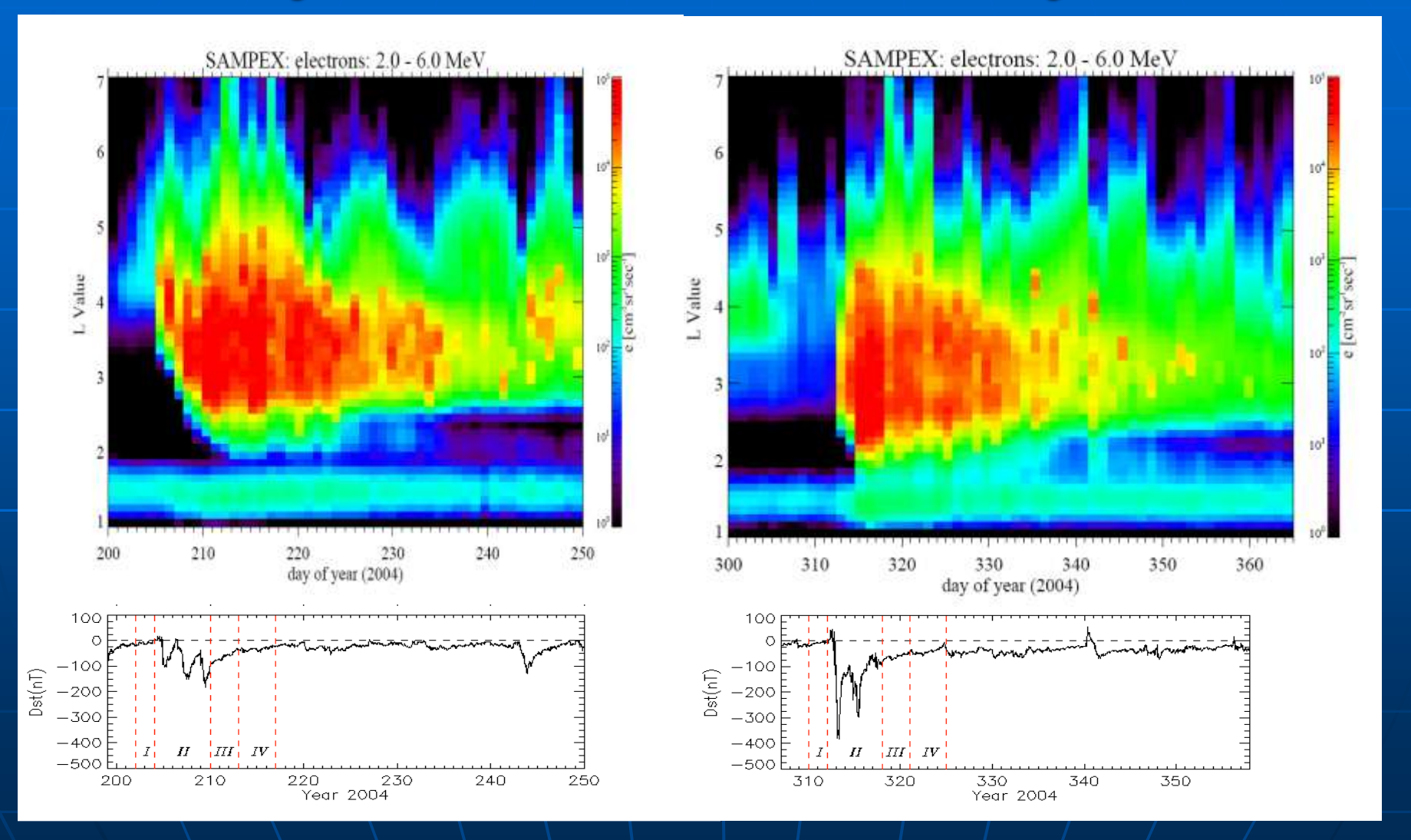
### SAMPEX 2-6 MeV for 03-05



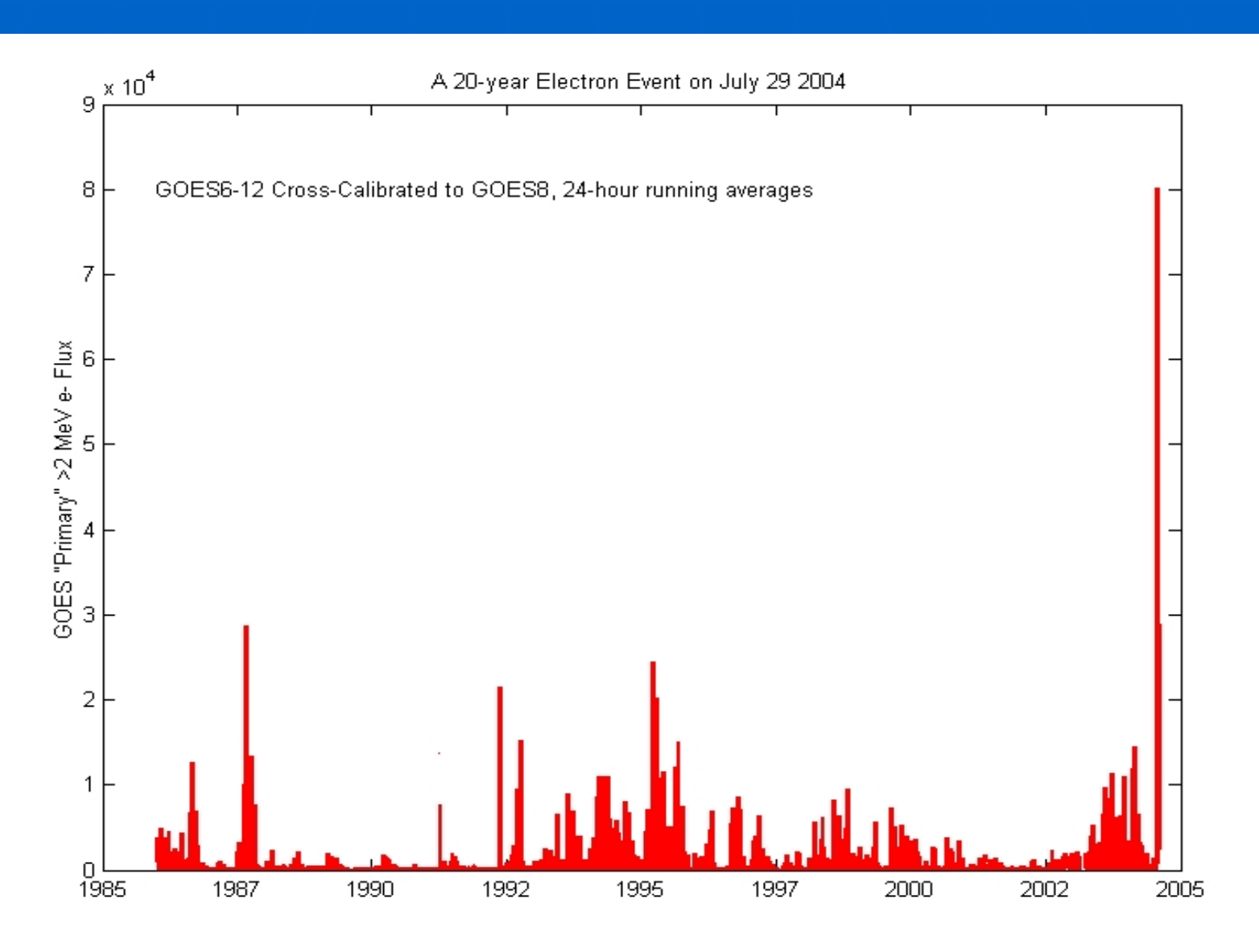
ig. 5. (a) Solar wind speed and (b) energetic electron fluxes for the period 2003 through 2005. he format of the data is closely analogous to that in Fig. 3.

Baker et al., 2008

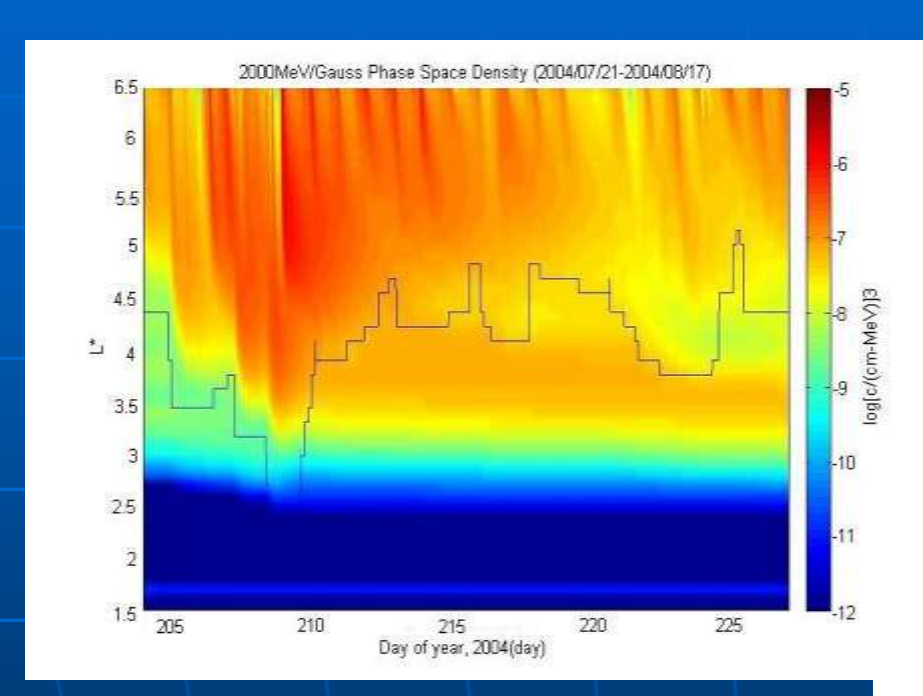
## July & Nov 04 Differ by SSC



### NOAA GOES > 2 MeV el flux



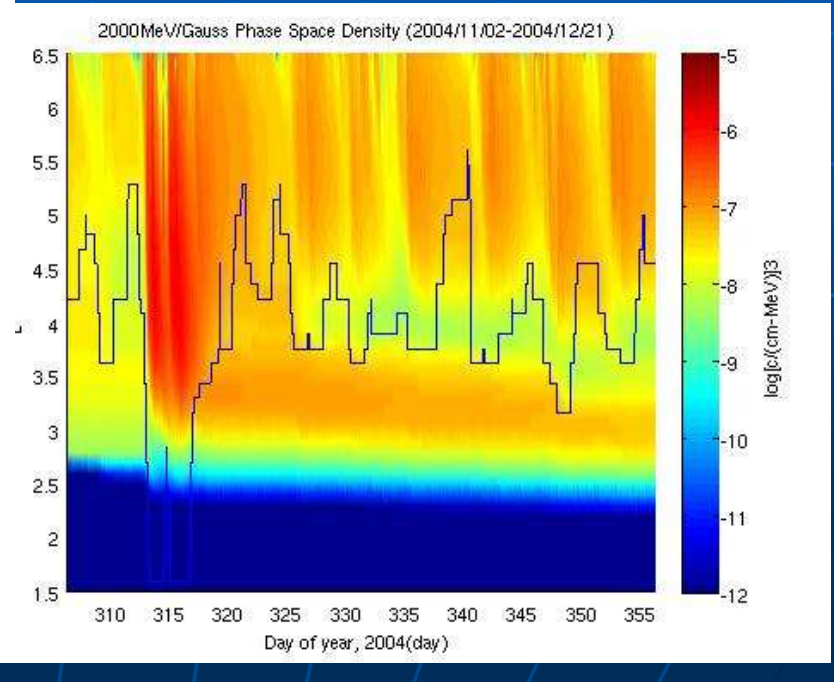
### Radial Diffusion for July & Nov 04



July 04 triple-storm

$$\frac{df}{dt} = L^{*2} \frac{\partial}{\partial L^{*}} \left[ D_{ll} L^{*-2} \frac{\partial f}{\partial L^{*}} \right] - \frac{f}{\tau}$$

Nov 04 SSC storm  $\mu$ = 2000 MeV/G  $f(\mathbf{v},\mathbf{r};t) = f(\mu,K,\Phi) = j/p^2$ 



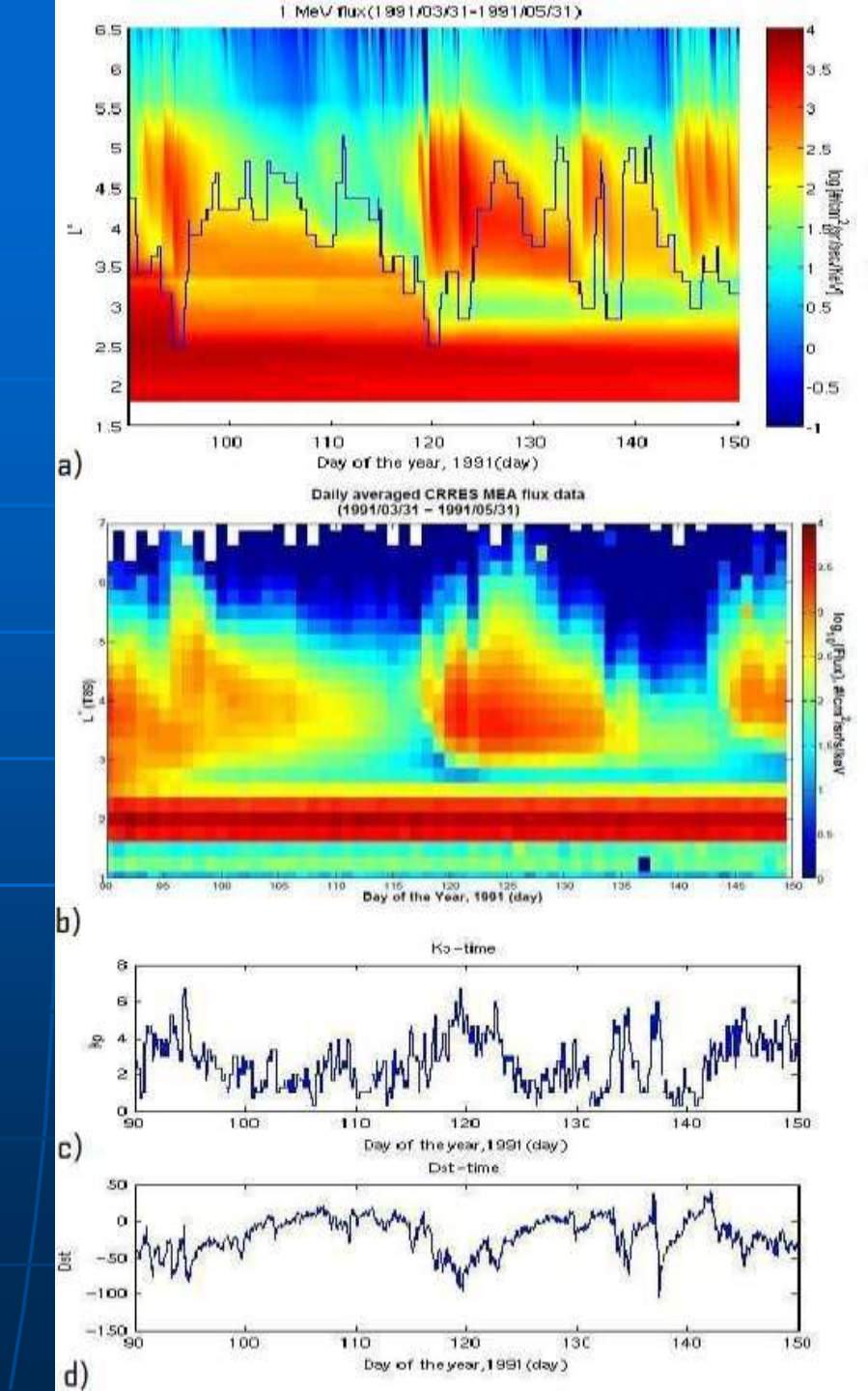
Kp-dependent D// and p'pause; lifetime inside (10 days) outside (Kp/3 days);

Dynamic outer boundary from LANL PSD

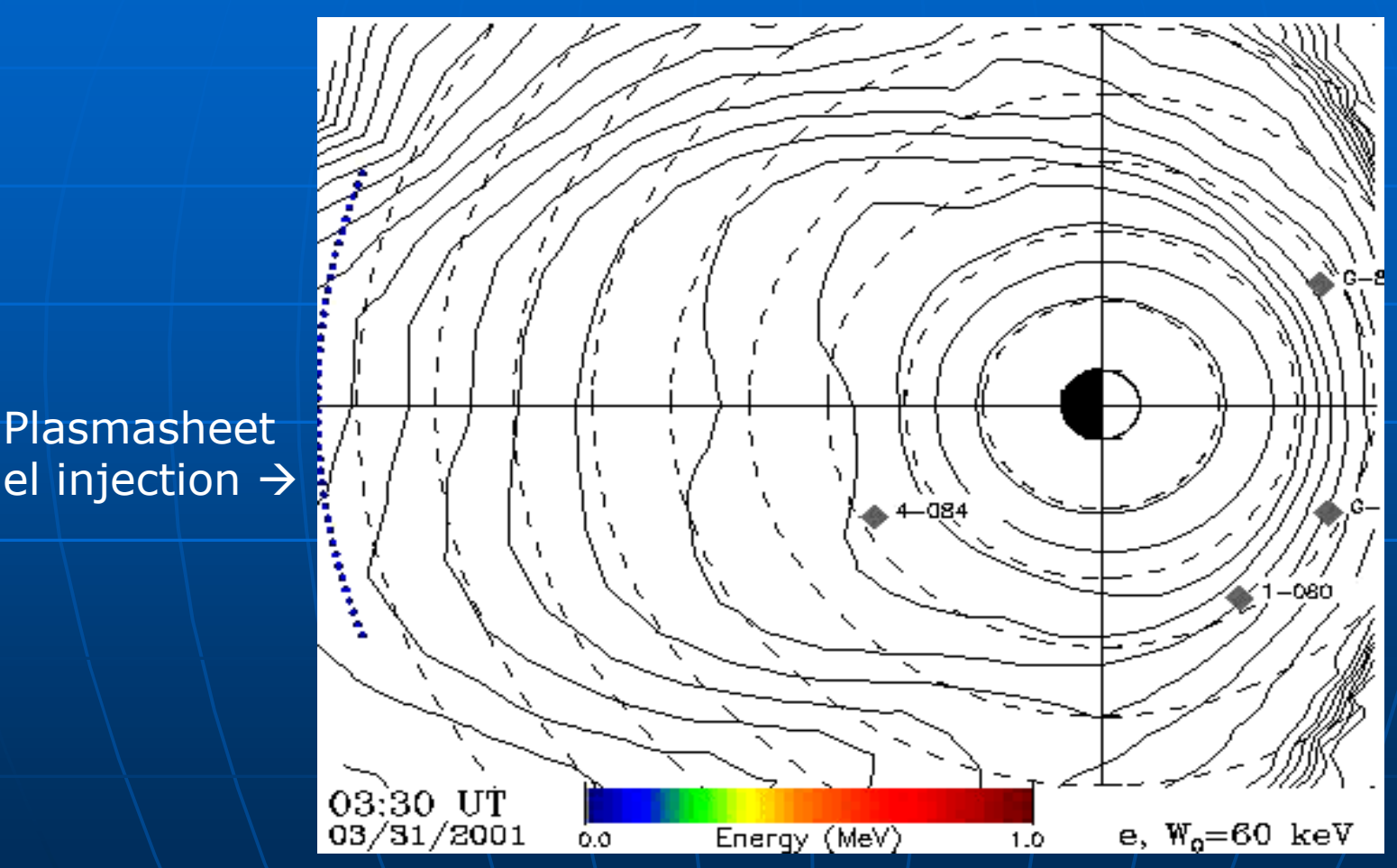
#### Radial Diffusion-CRRES Data Comparison

- 2-months following
   March 1991 prompt injection
- Recurring high speed streams
- Recovery of slot region as plasmapause penetrates to low L

1 MeV fluxes, interpolated from PSD at fixed Mu



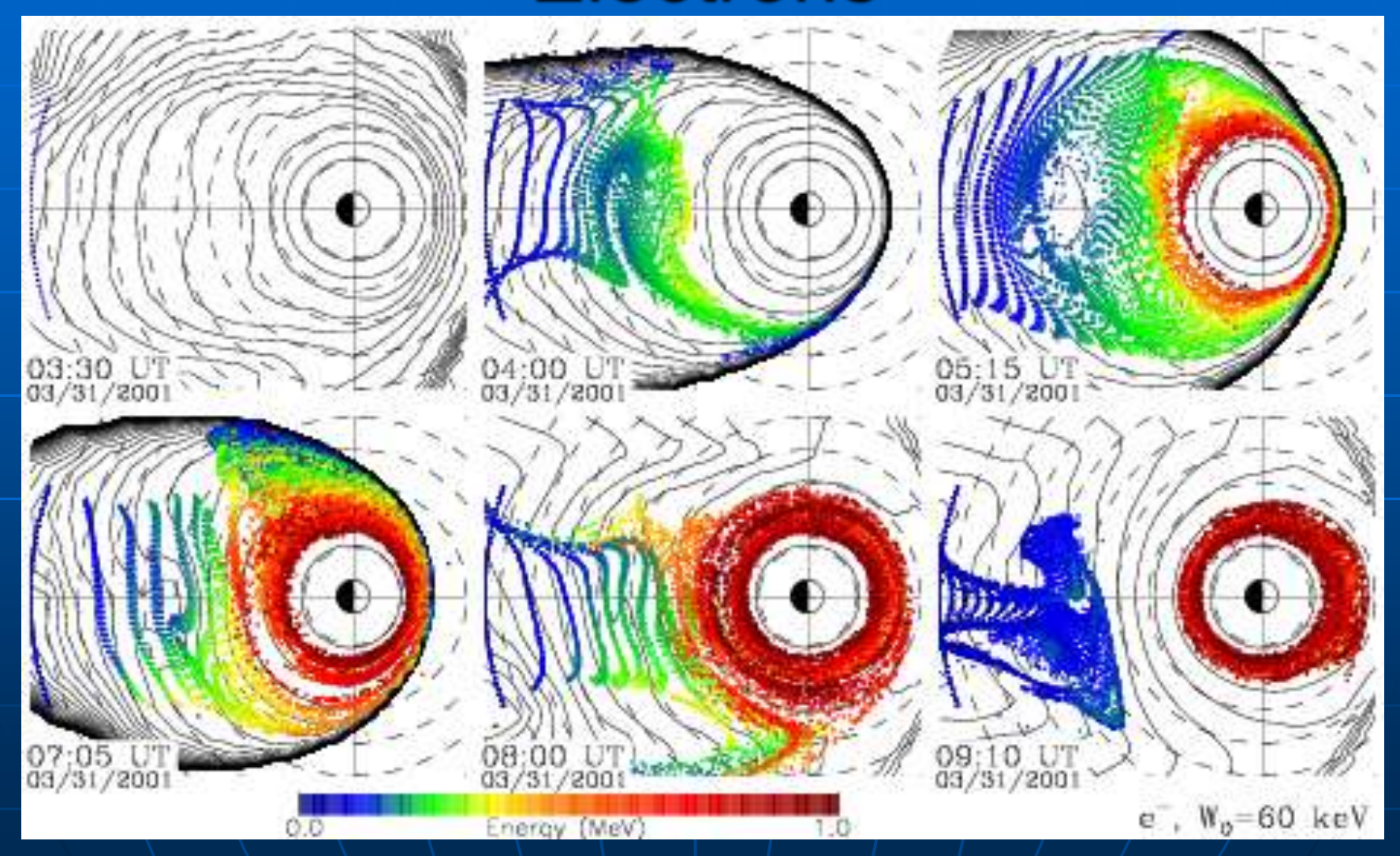
## MHD Fields Inject RadBelt Electrons



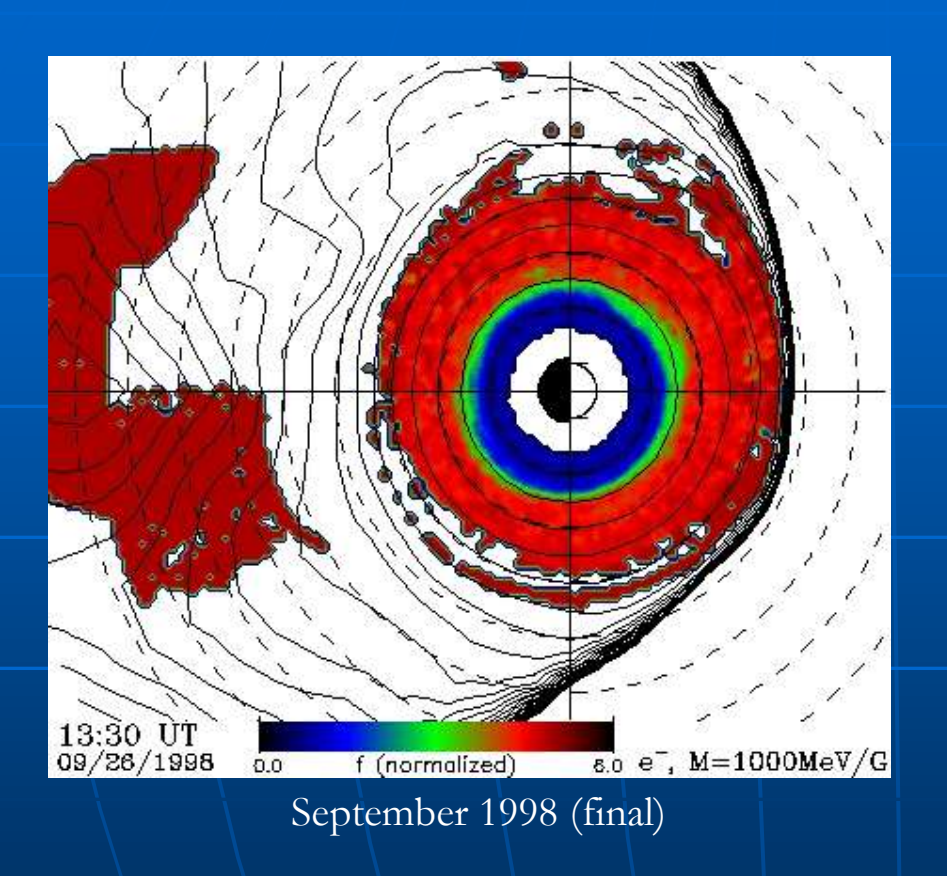
Plasmasheet

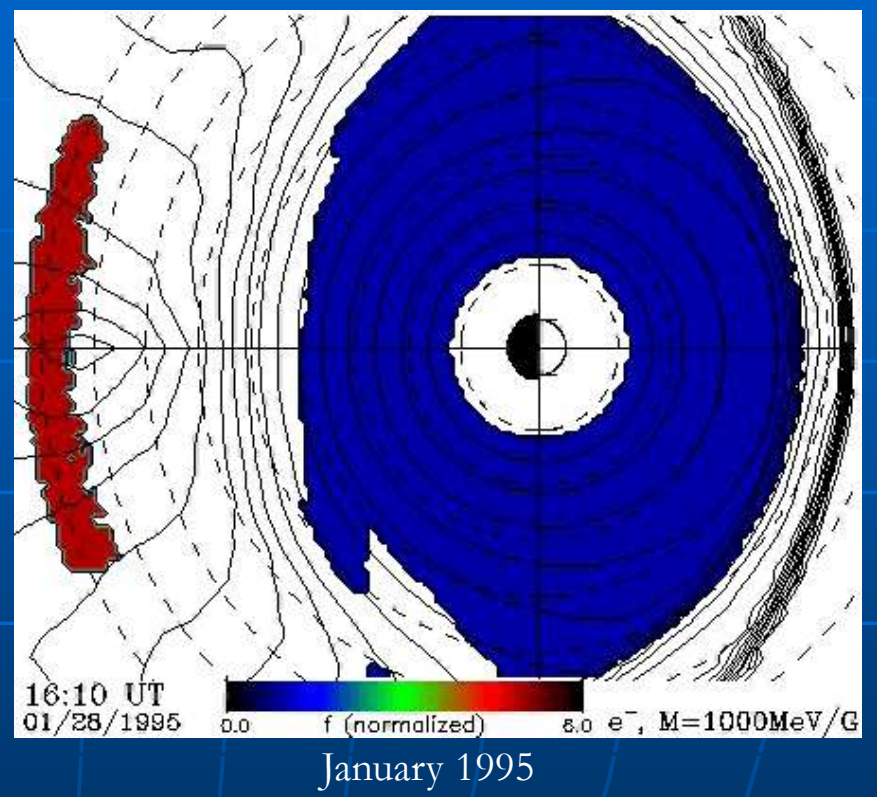
Elkington et al., JASTP, 2004

# MHD Fields Injection of RadBelt Electrons



### f calculations for other storms...

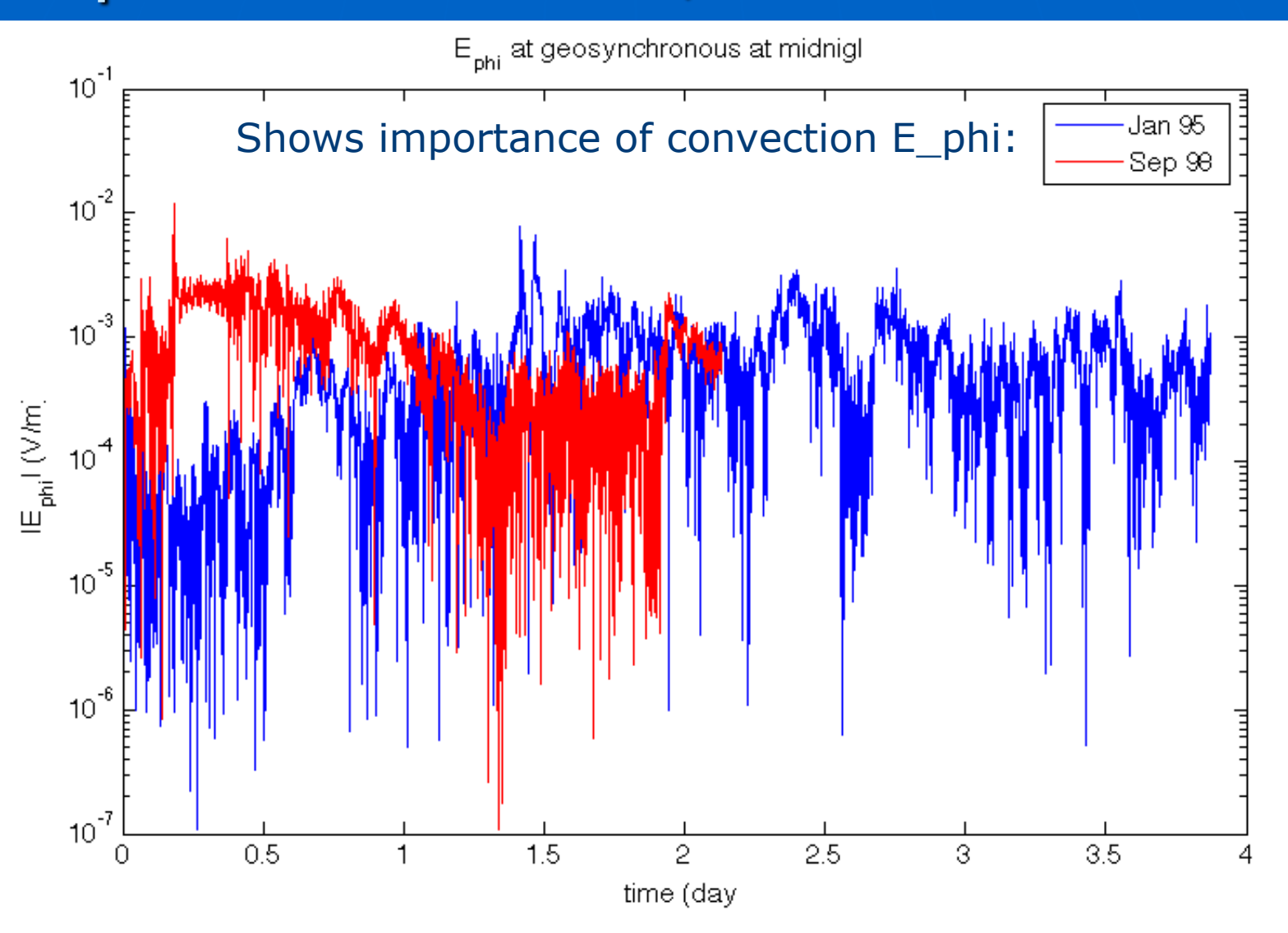




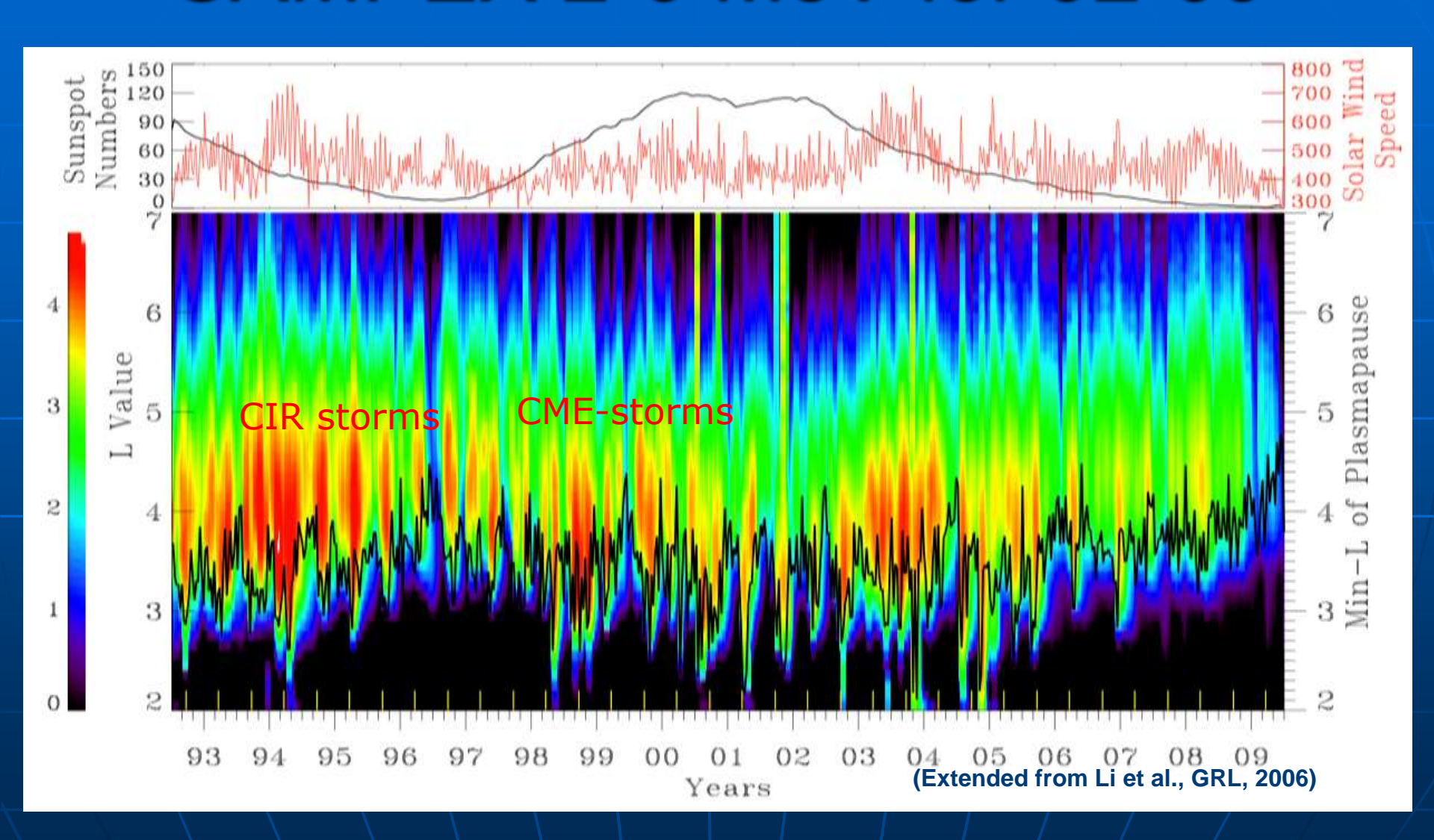
- •The (big) September 1998 storm shows a significant change in trapped PSD as a result of coupling to the plasmasheet.
- •The more moderate storm of January 1995 showed almost no coupling with the plasmasheet.

  Elkington et al., 2008

### Sep 98 CME Storm, Jan 95 Substorm

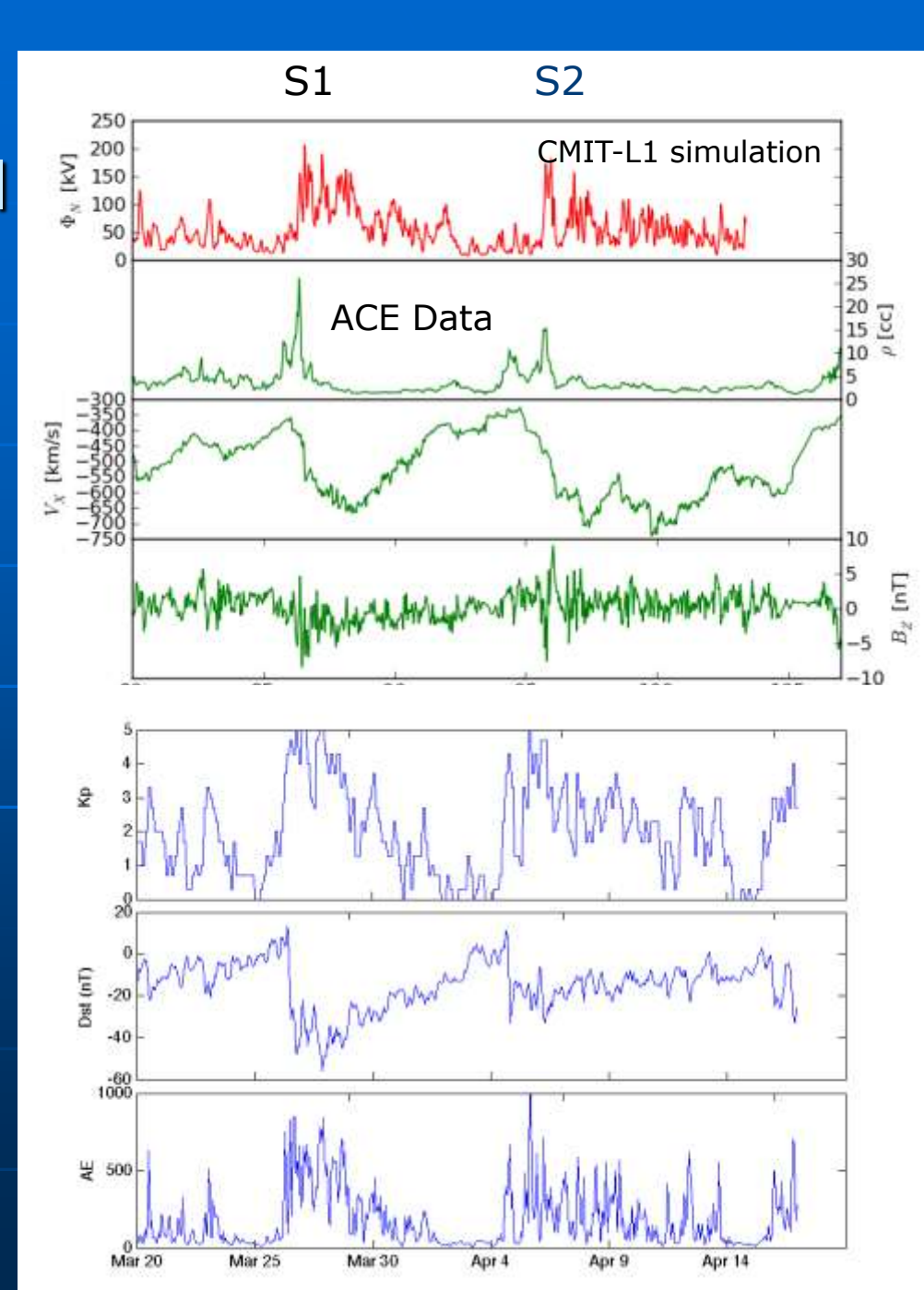


### SAMPEX 2-6 MeV for 92-09

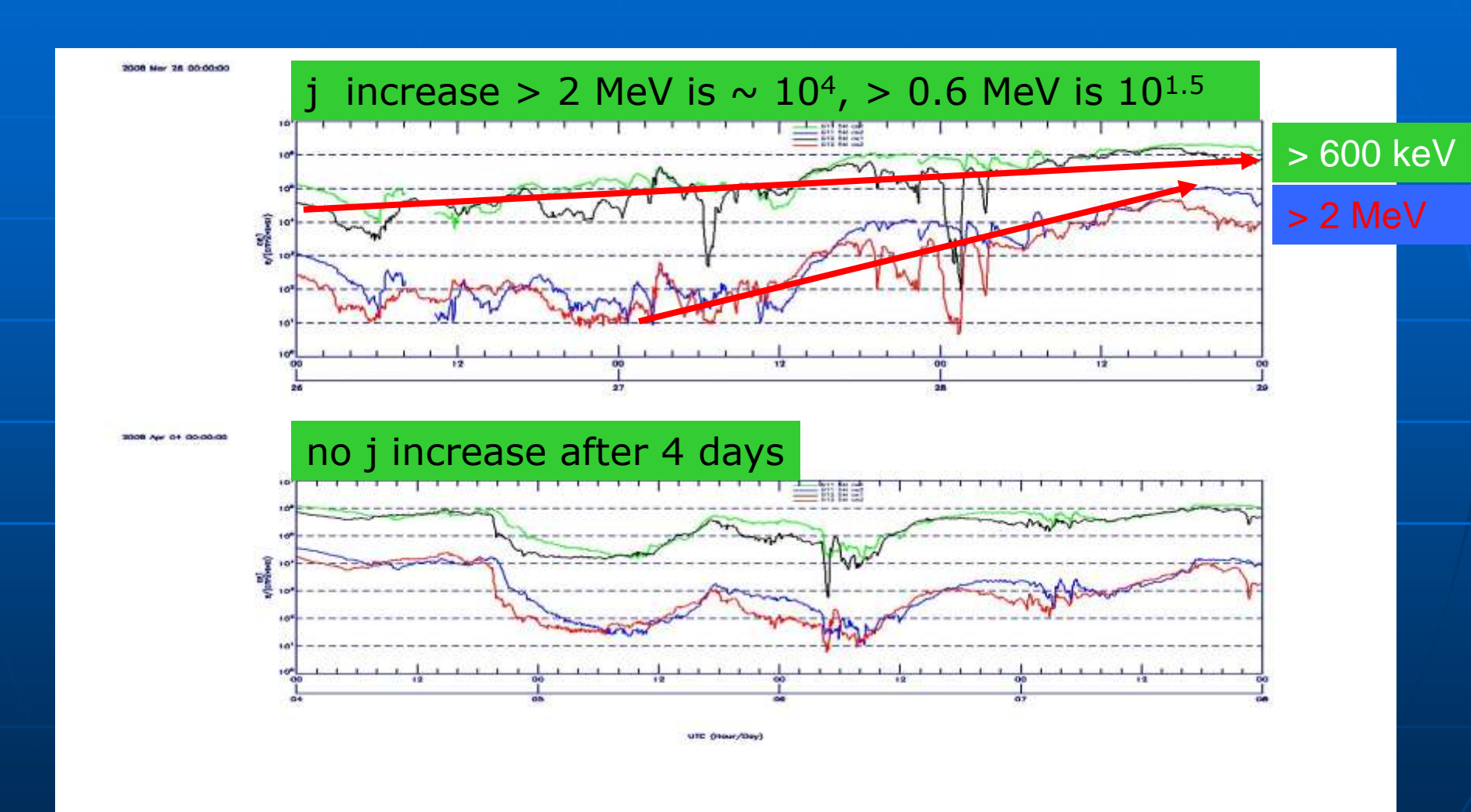


# CIR Stream Interactions March-April 2008 Whole Heliosphere Interval

- Geospace response to each stream had distinct features
  - Stream 1 had higher Φ<sub>pc</sub> for longer than Stream 2 even though V<sub>x</sub> was lower
  - B<sub>z</sub> plays an important role in determining geoeffectiveness of streams
  - Carrington Rotation 2068



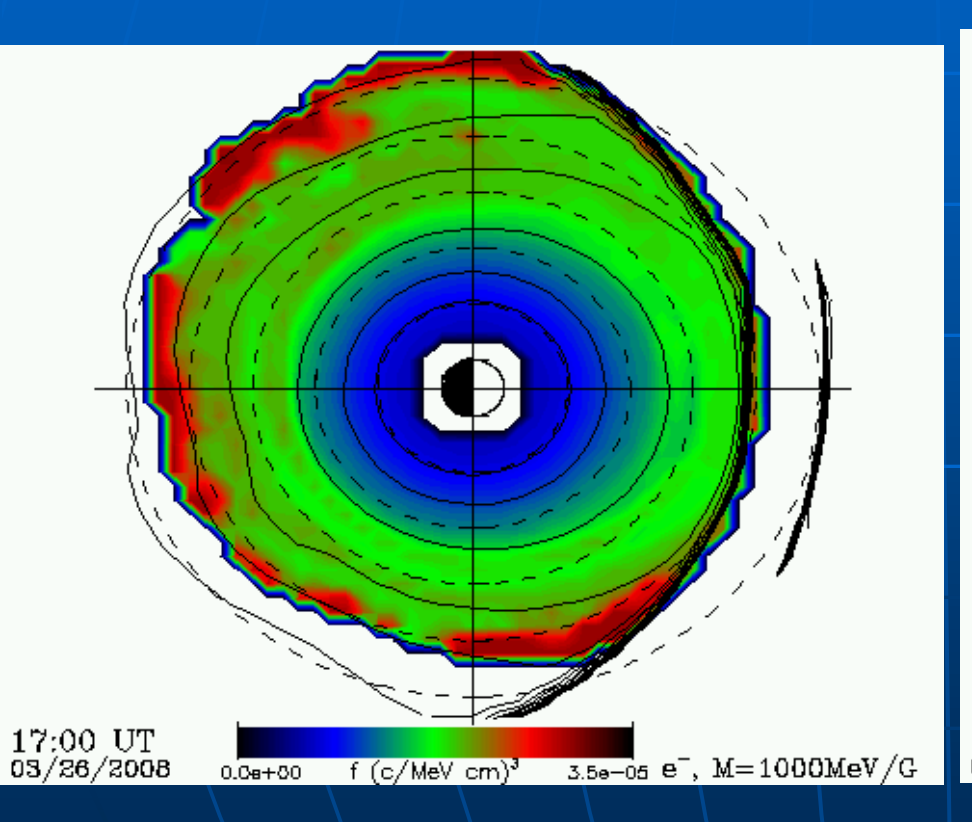
### Stream 1&2 GOES Electrons

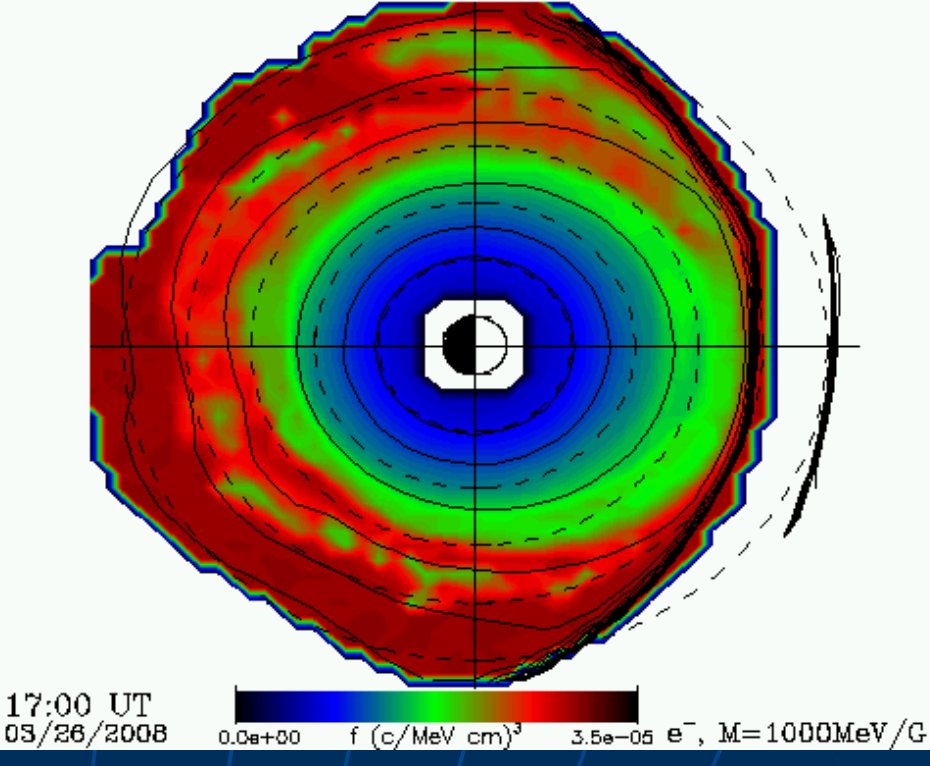


### 2D-Plasmasheet Injection

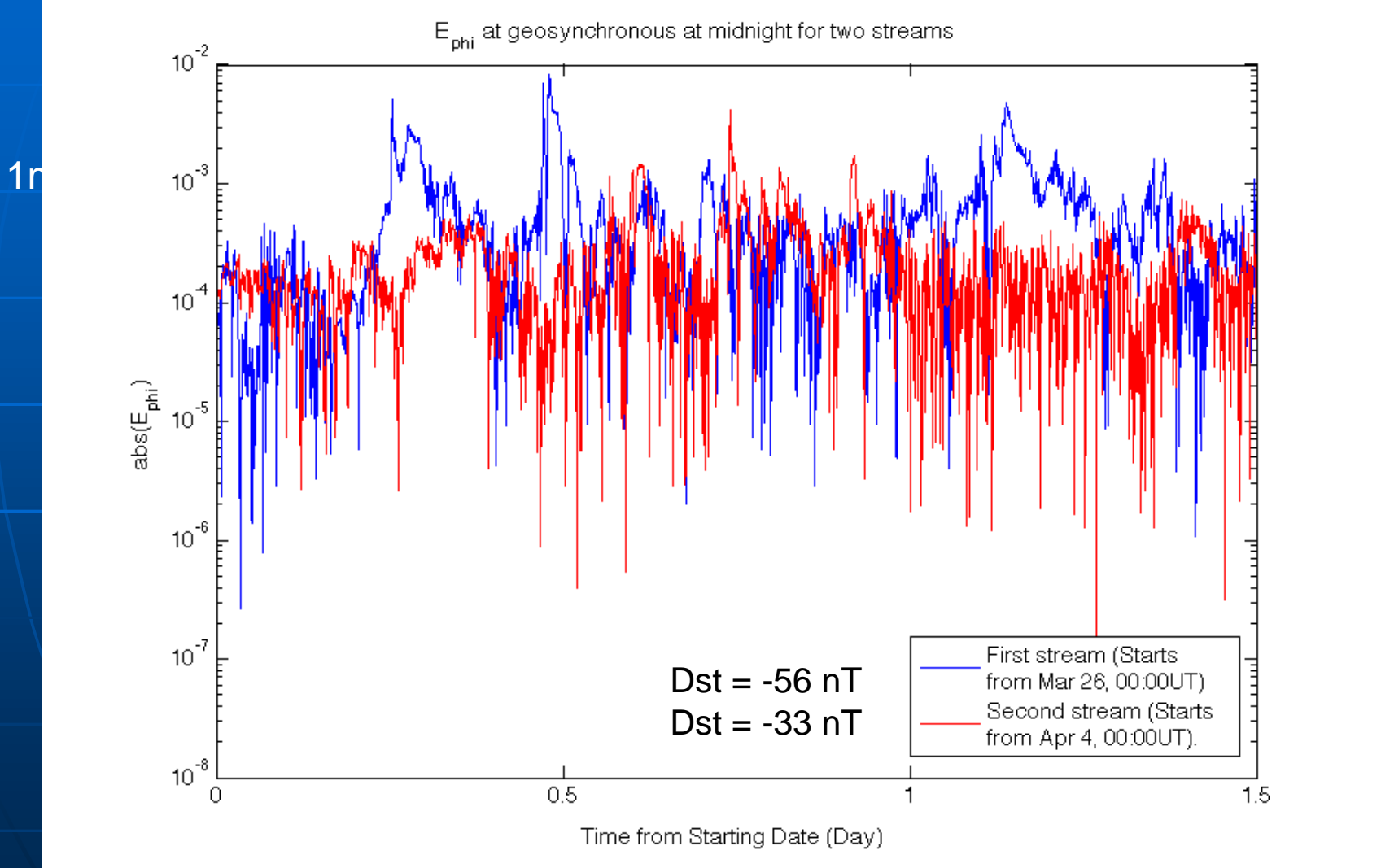
Trapped only: losses

Trapped + P'sheet Injection

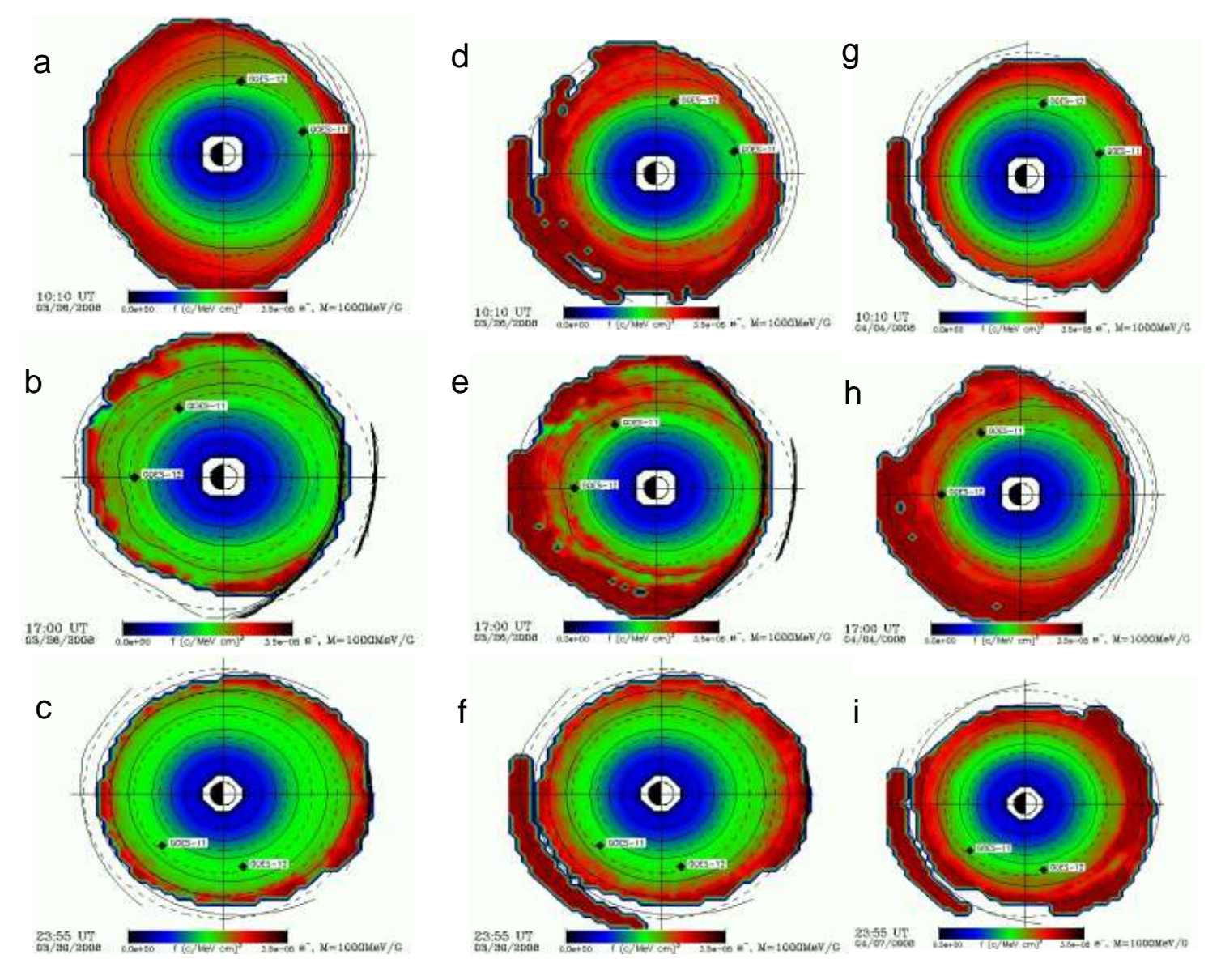




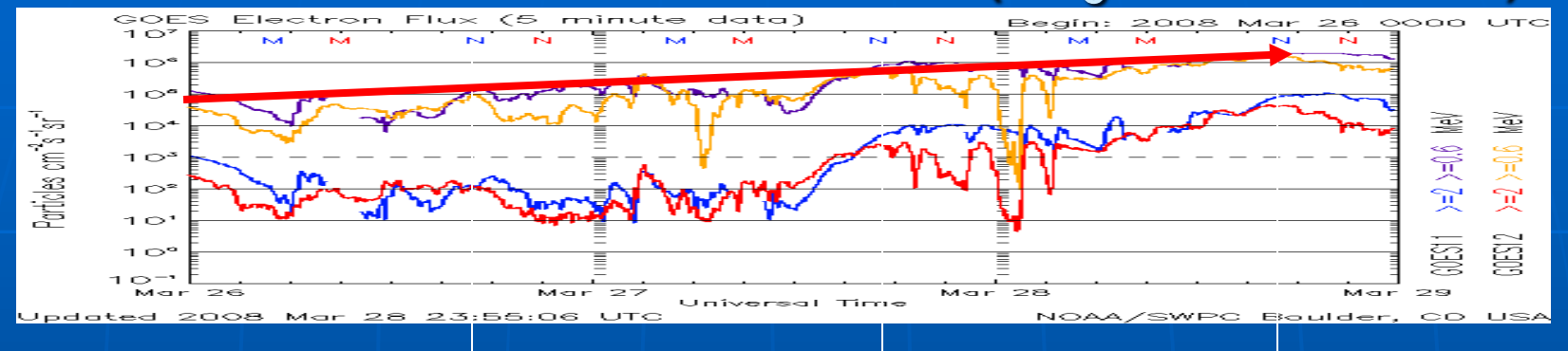
# E<sub>φ</sub> at GEO Determines Efficiency of Plasmasheet Injection

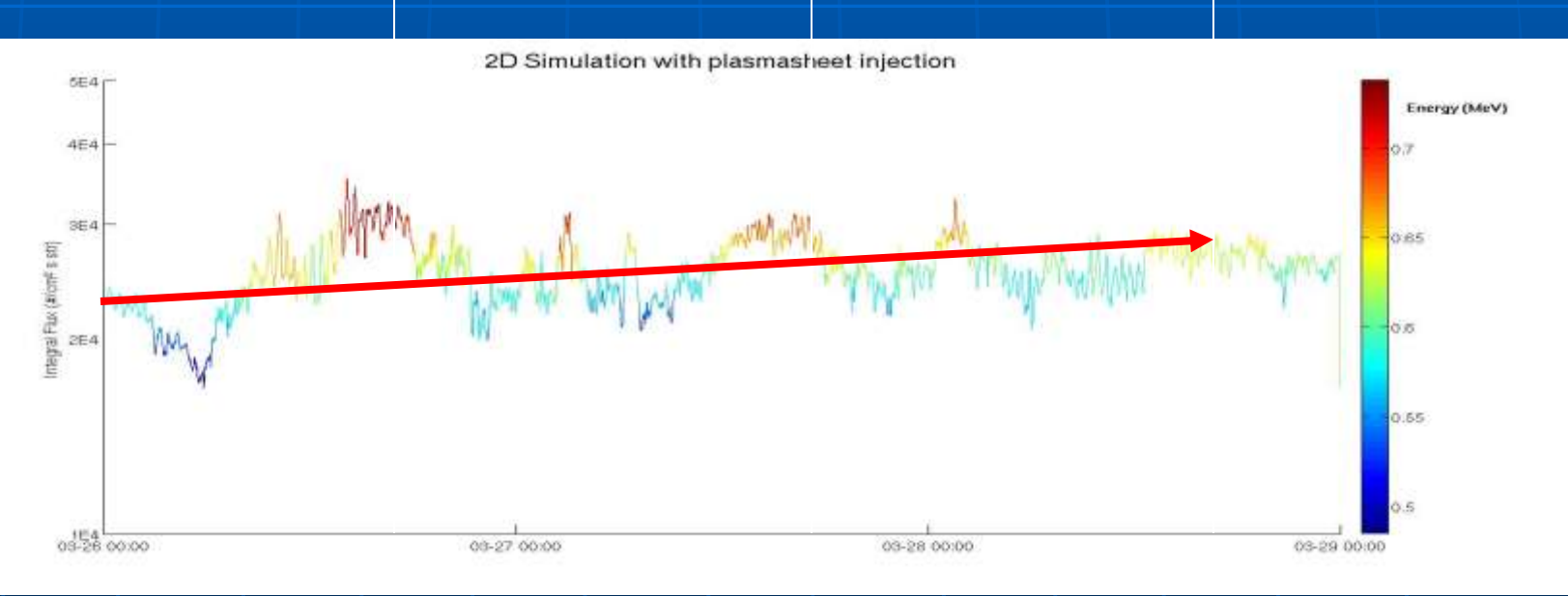


### 2D PSD: Stream1 Stream2

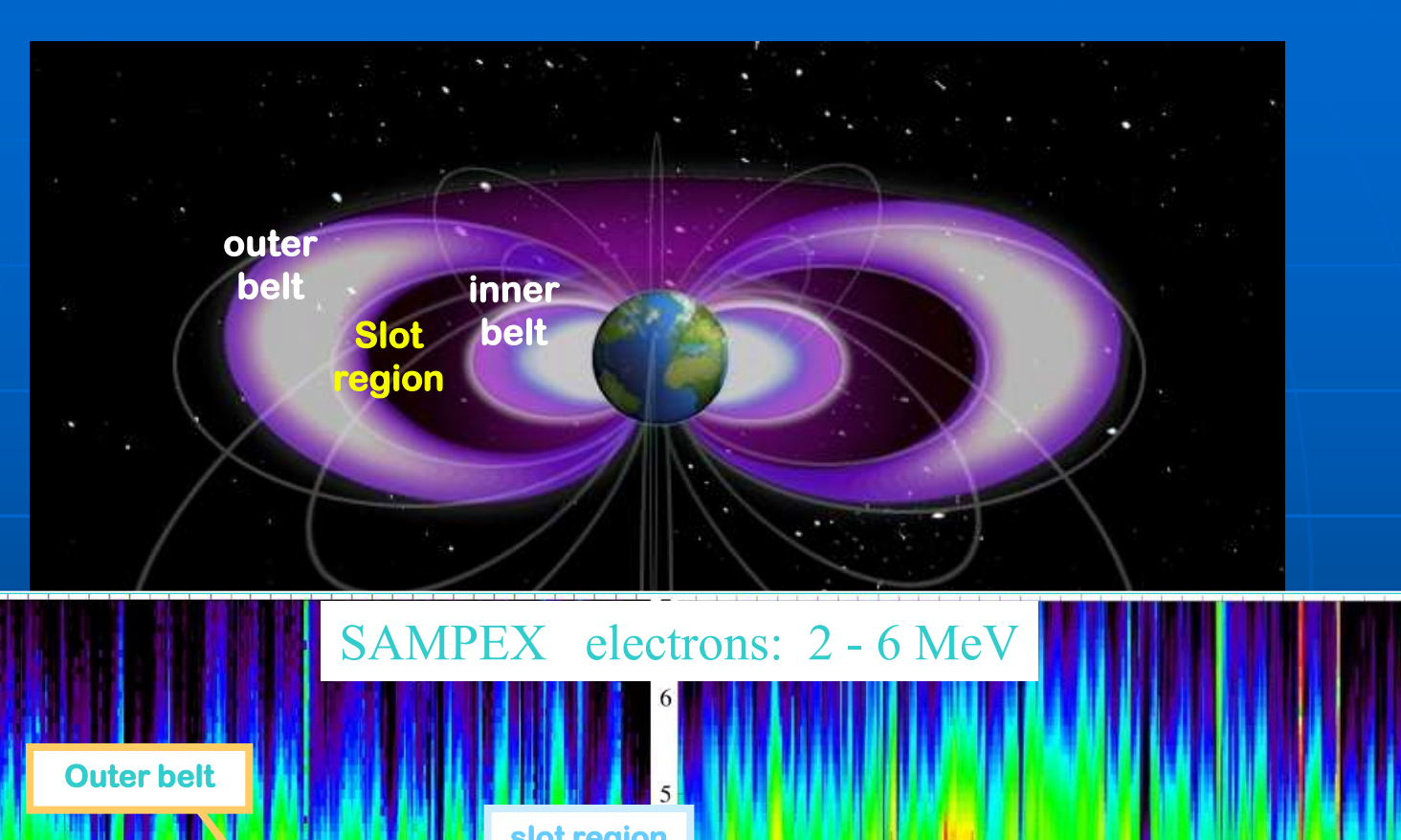


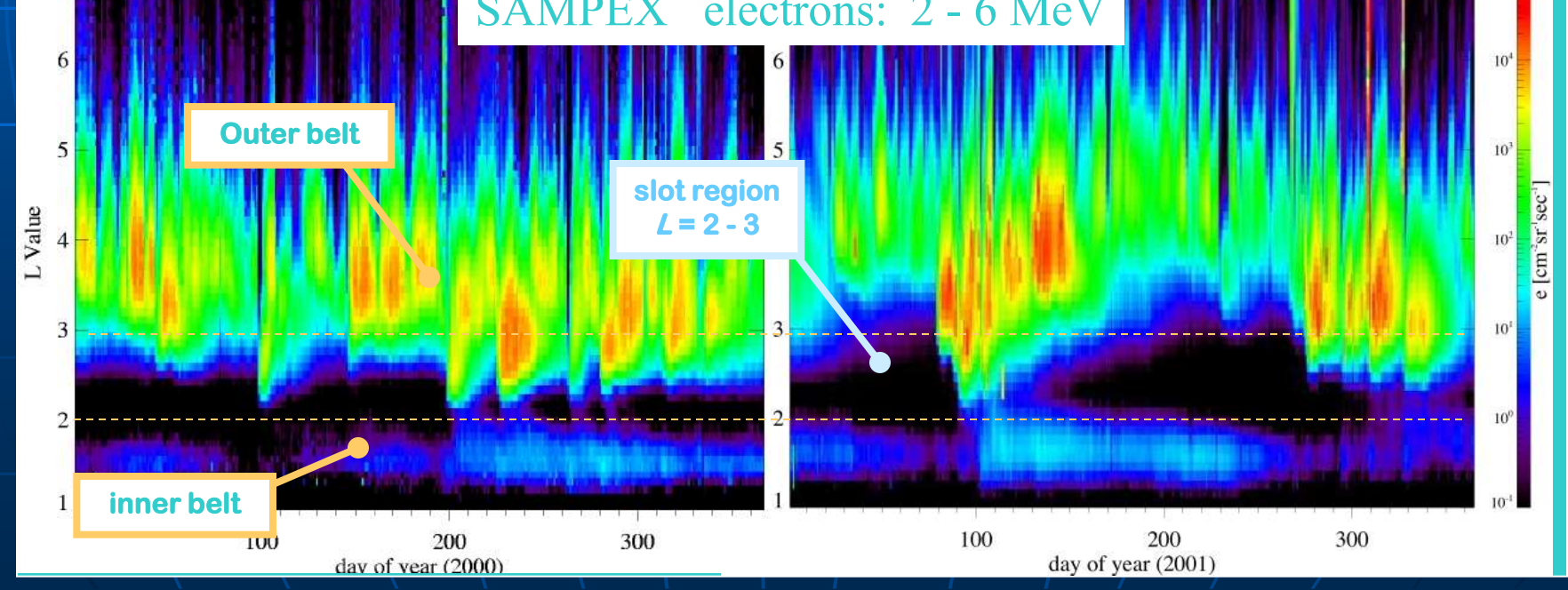
## Flux and Energy Increase at GOES 12 for Stream 1 at 1000 MeV/G ( $W_0 = 600 \text{ keV}$ )





#### Slot region variability tied to plasmapause

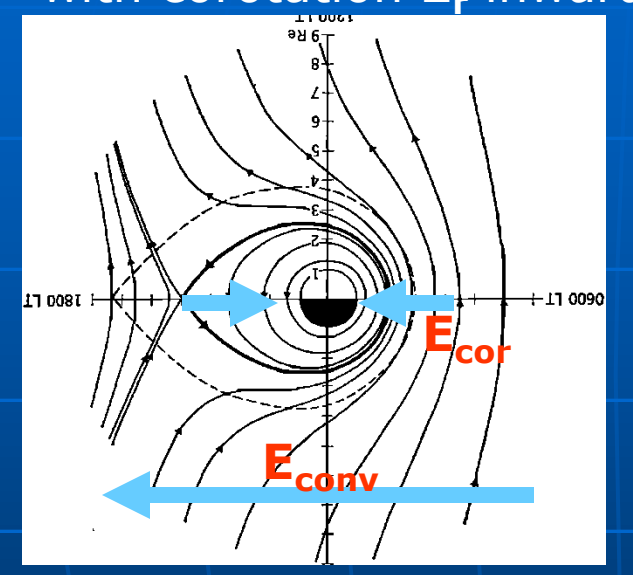




## Plasmapause explanation

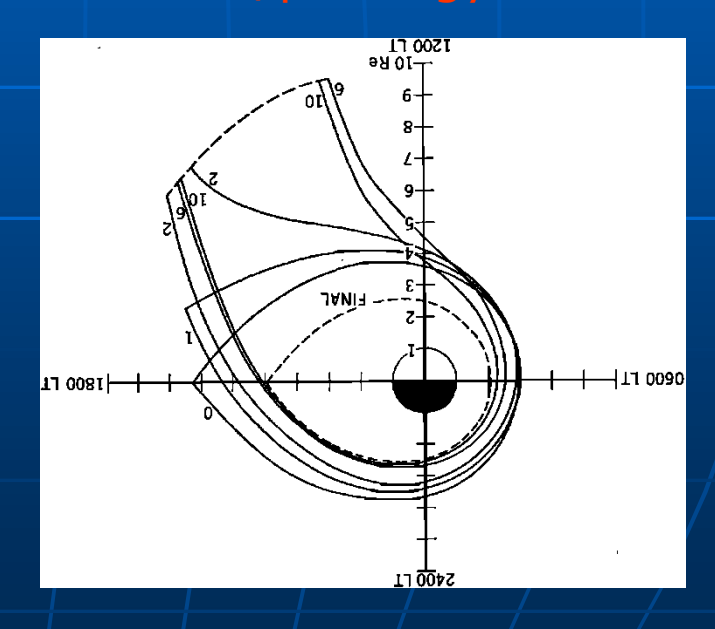
Balance convection  $\mathbf{E_0} \rightarrow$  assume uniform dawn-dusk with corotation  $\mathbf{E_r}$  inward, oppose at dawn moves p'pause inward and

reinforce at dusk moves p'pause outward



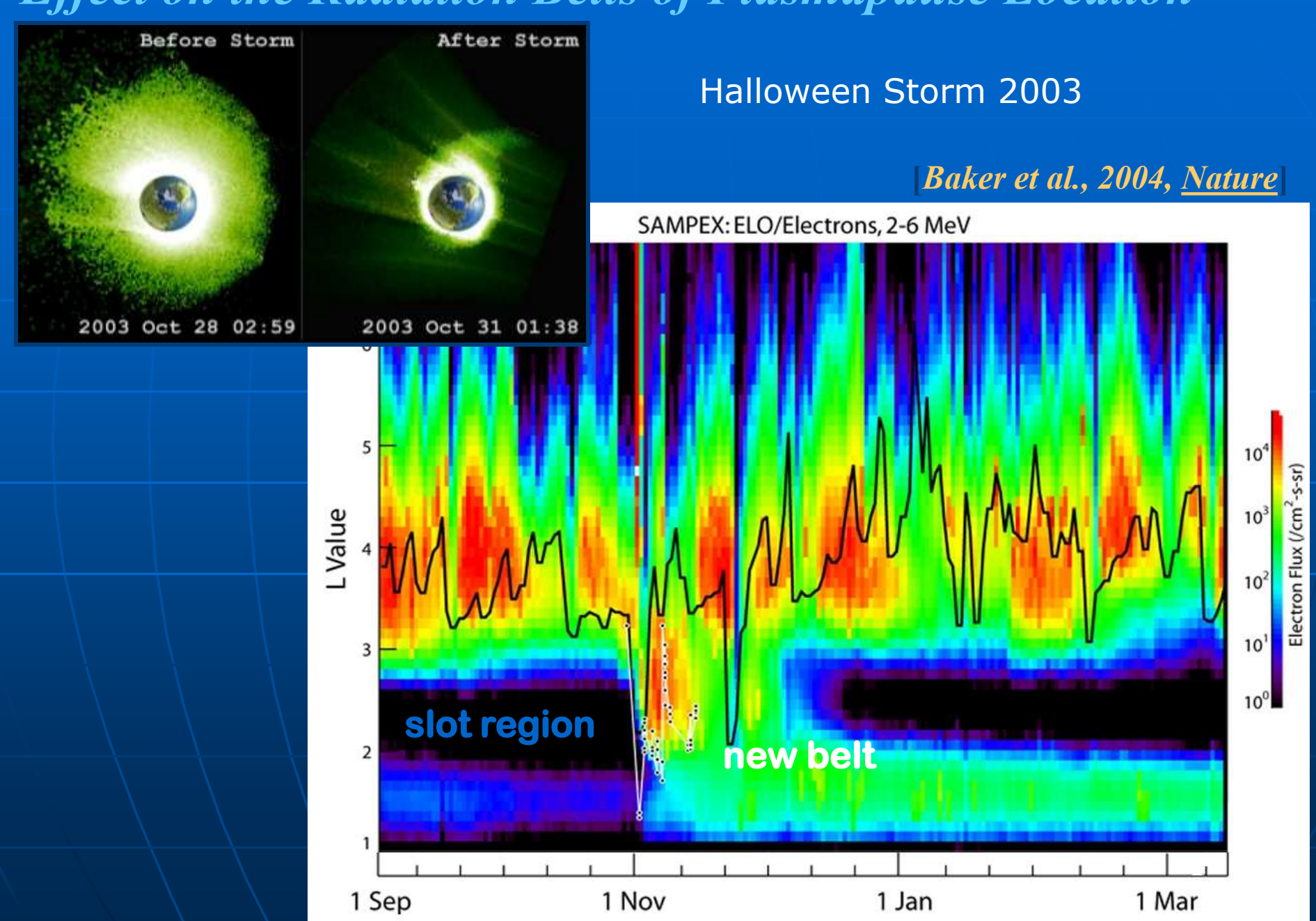
Related separatrix between convecting and grad-B drifting plasma: Alfven layer Depends on el/p energy and local B

Dayside plume forms when  $\mathbf{E_0}$  increases, p'pause moves inward

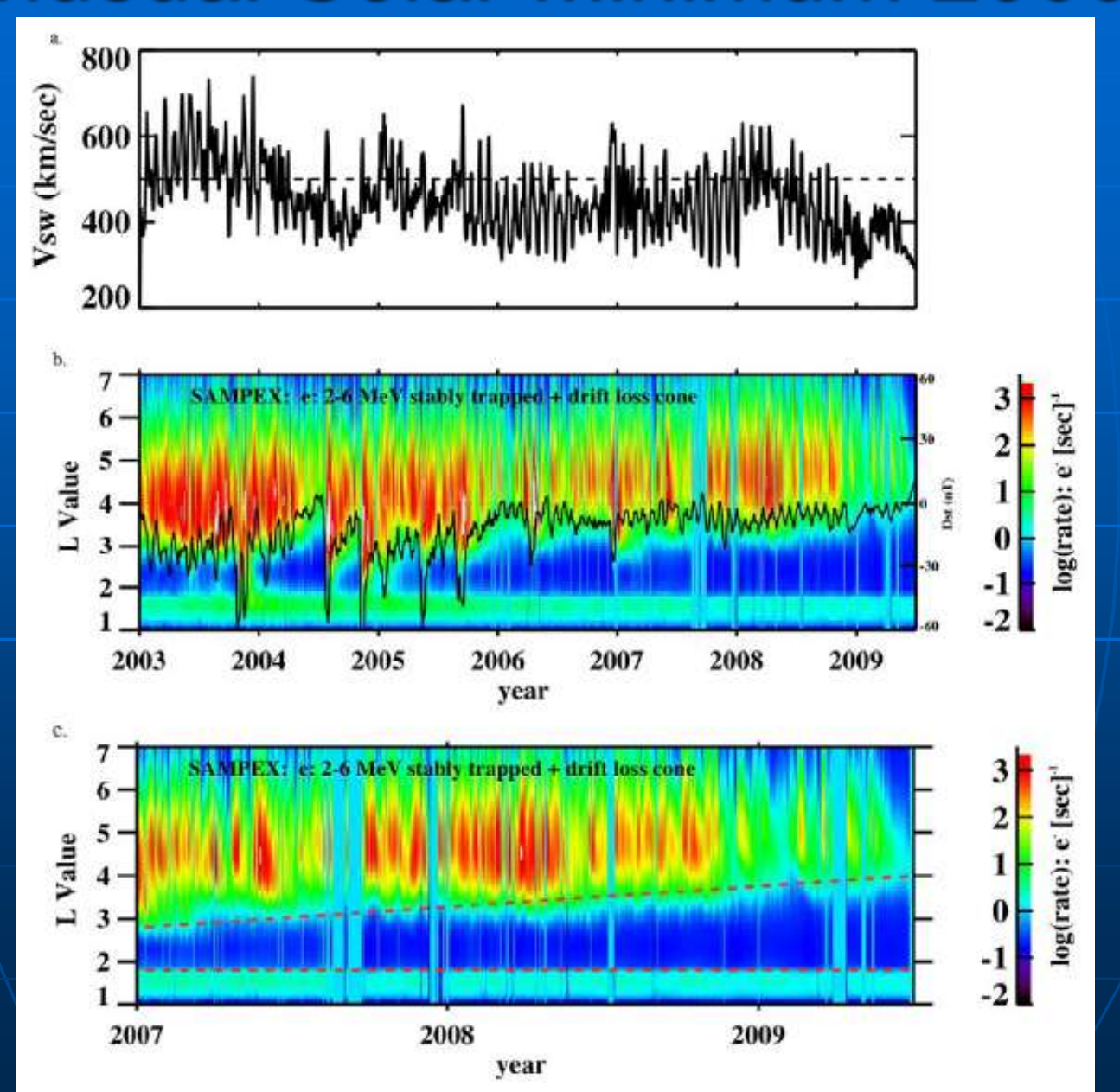


Grebowsky, JGR, 1970

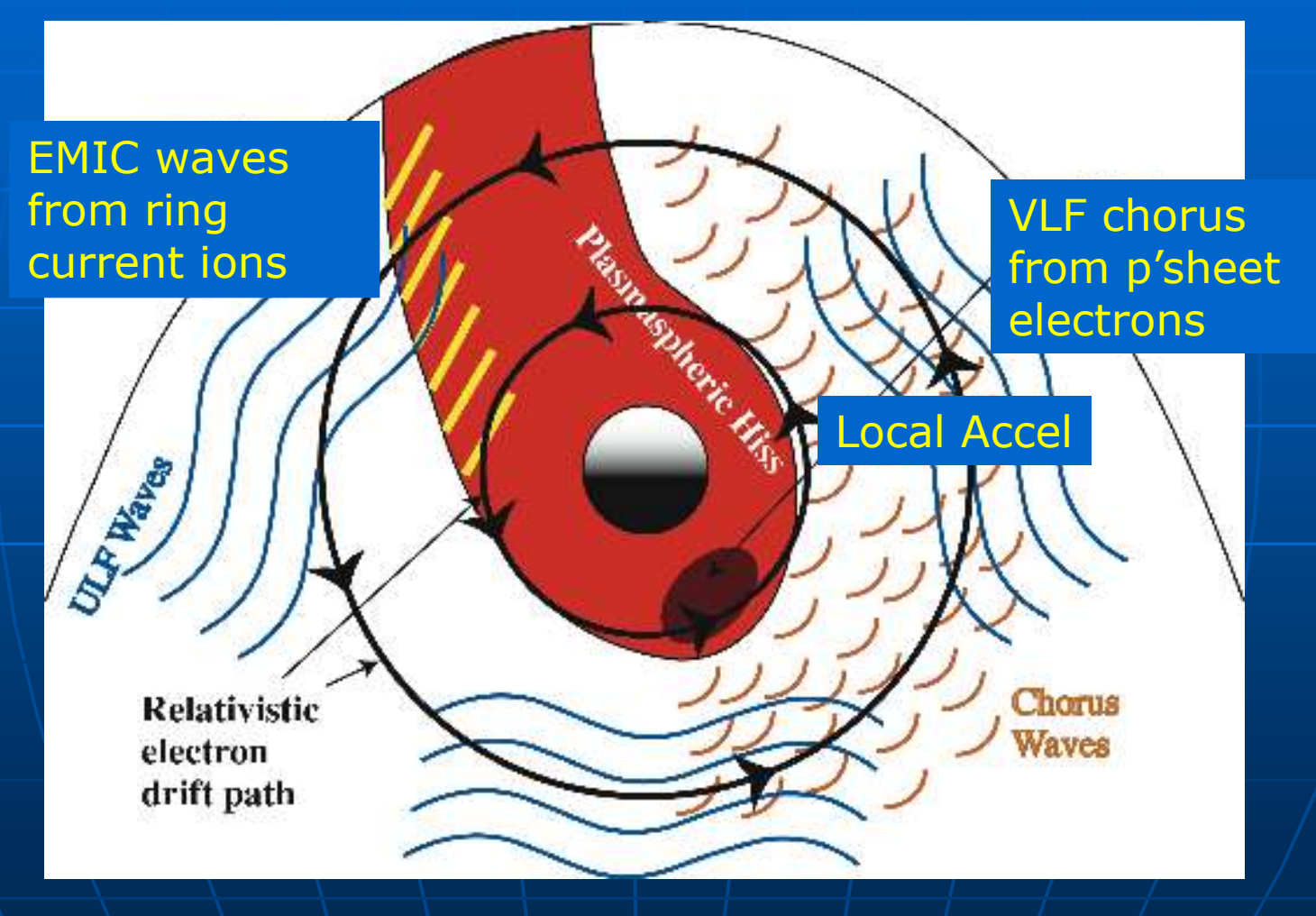
#### Effect on the Radiation Belts of Plasmapause Location



## **Unusual Solar Minimum 2009**

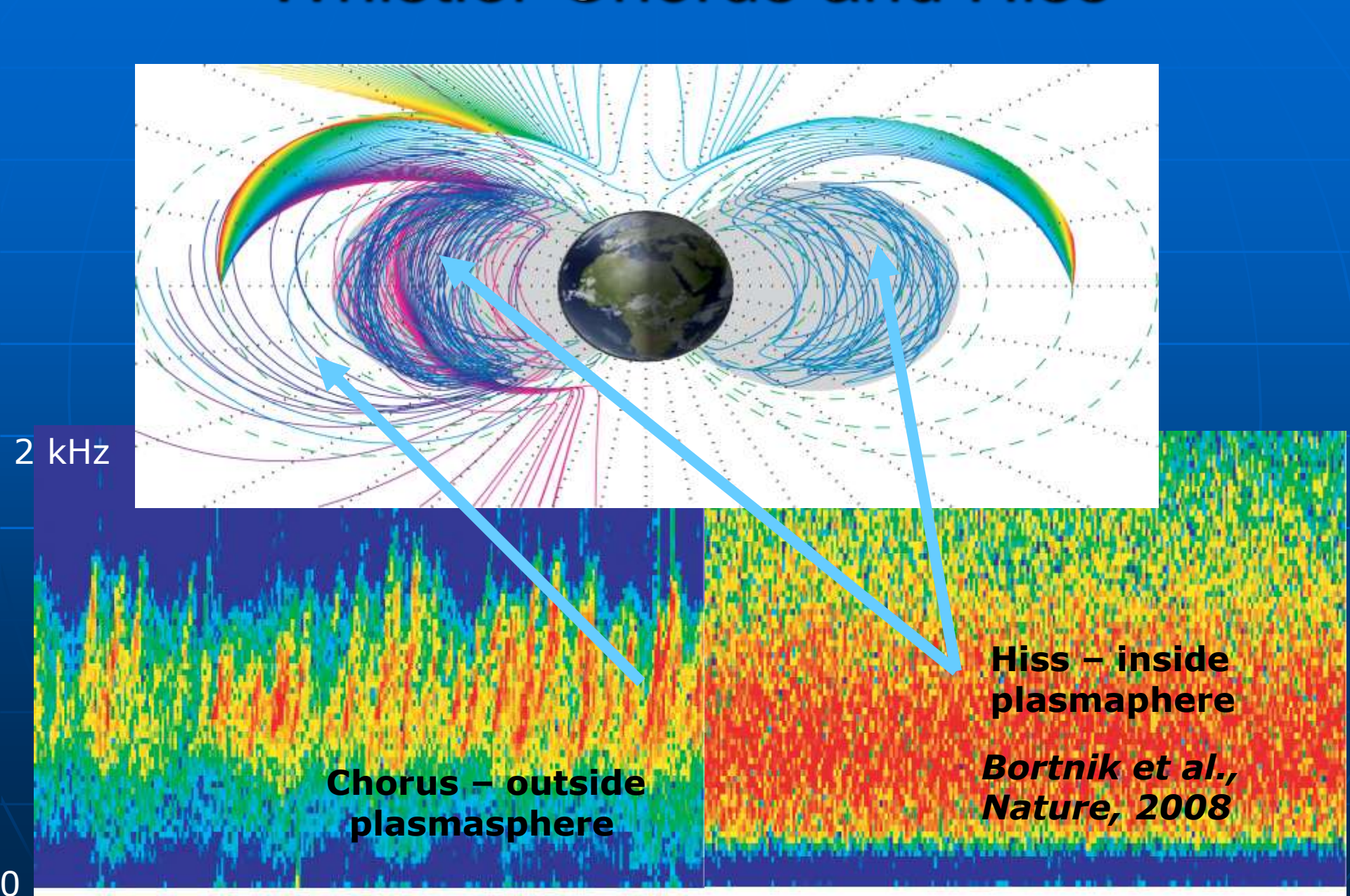


# Pitch Angle & Energy Diffusion Internal Loss & Source

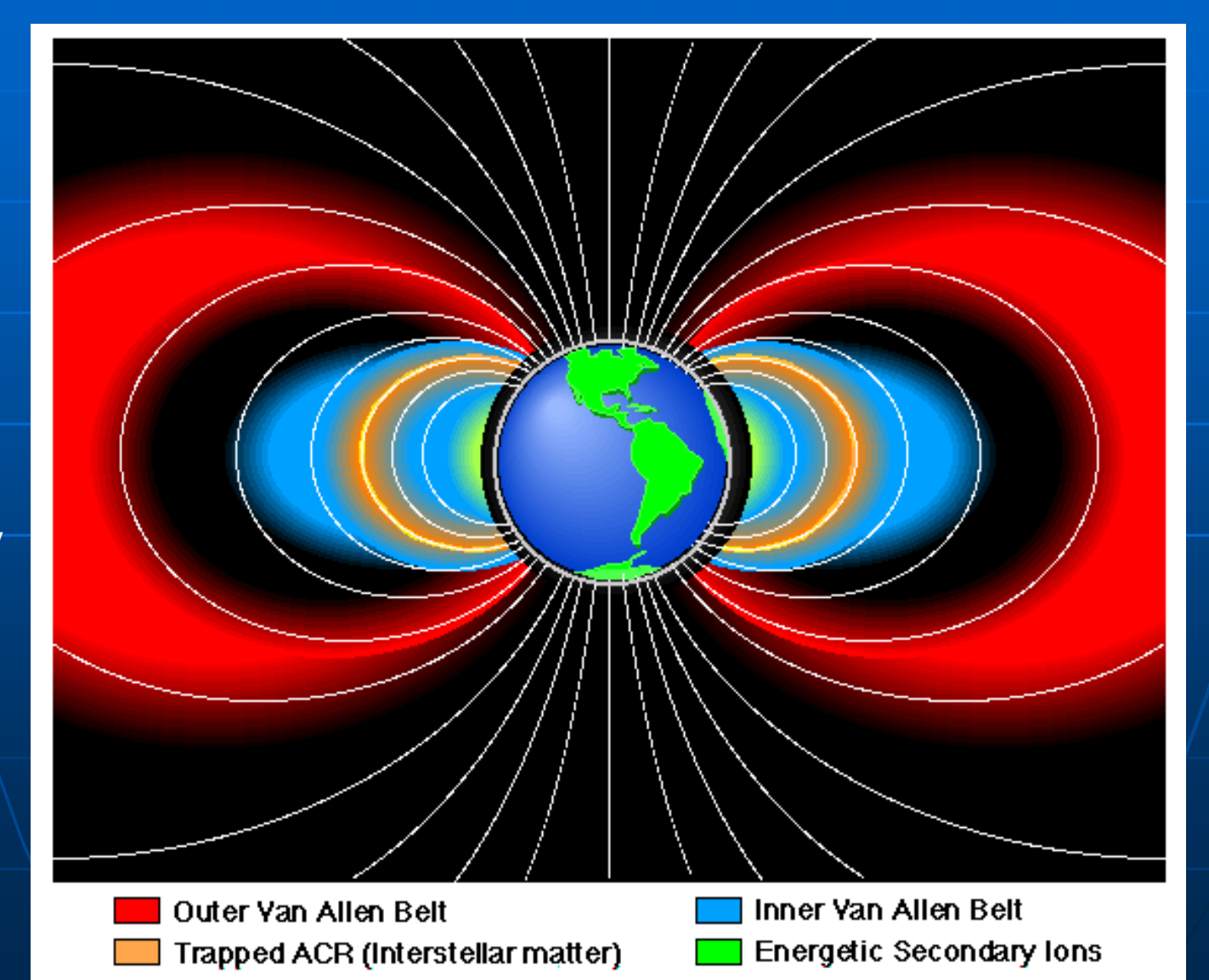


After Summers et al., 1998

## Whistler Chorus and Hiss

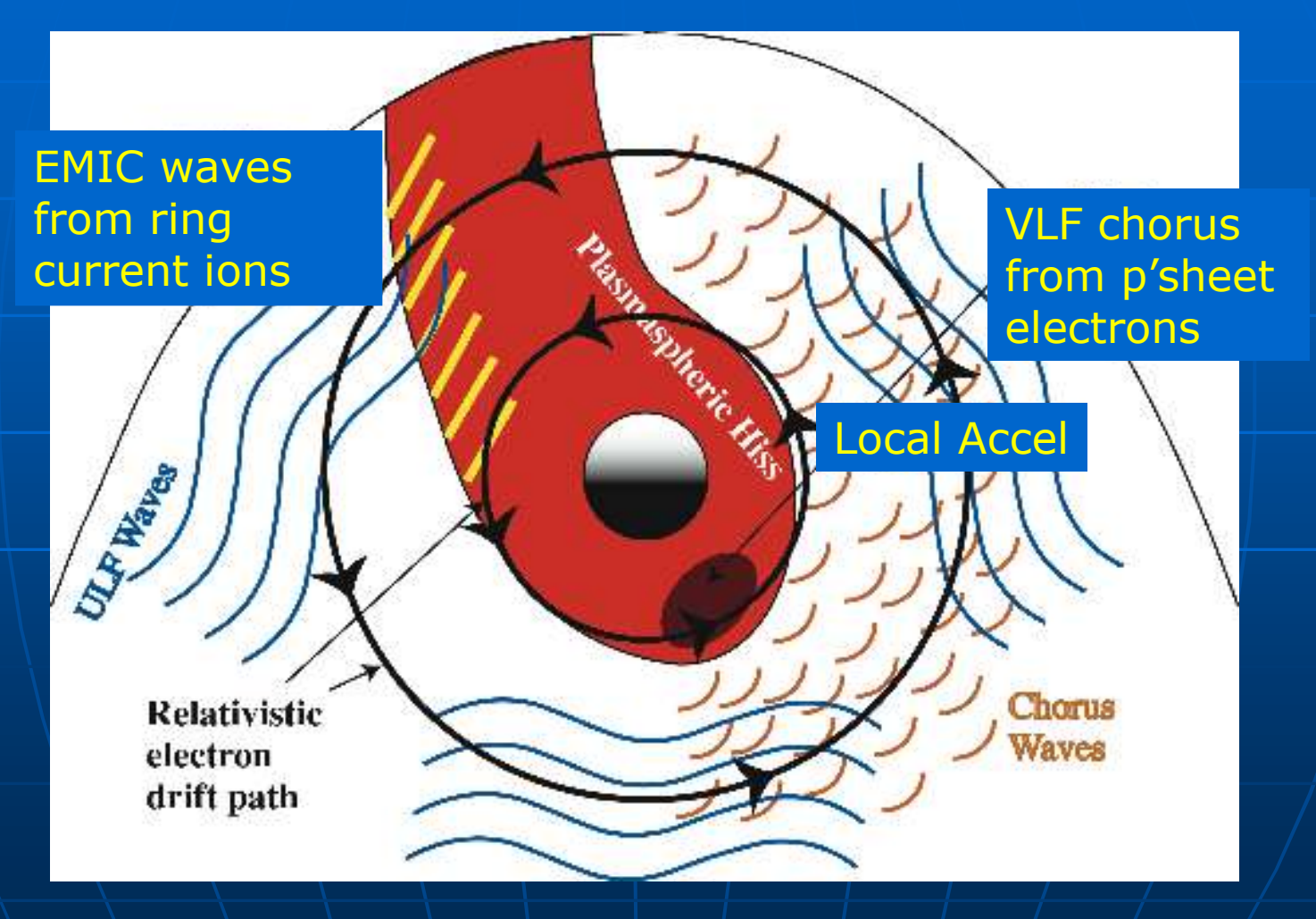


## Slot Region Due to Hiss



ρ ~ B/grad Bdeterminestrapping boundary

# Pitch Angle & Energy Diffusion Internal Loss & Source

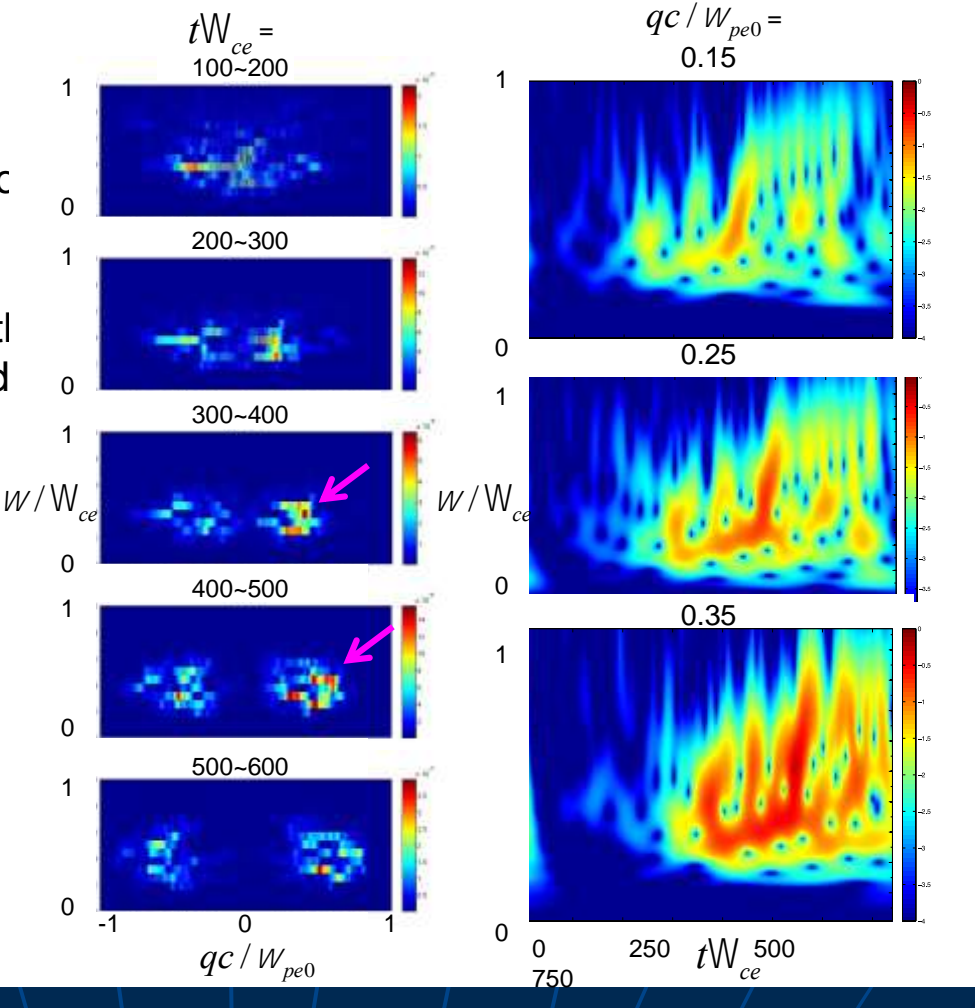


After Summers et al., 1998

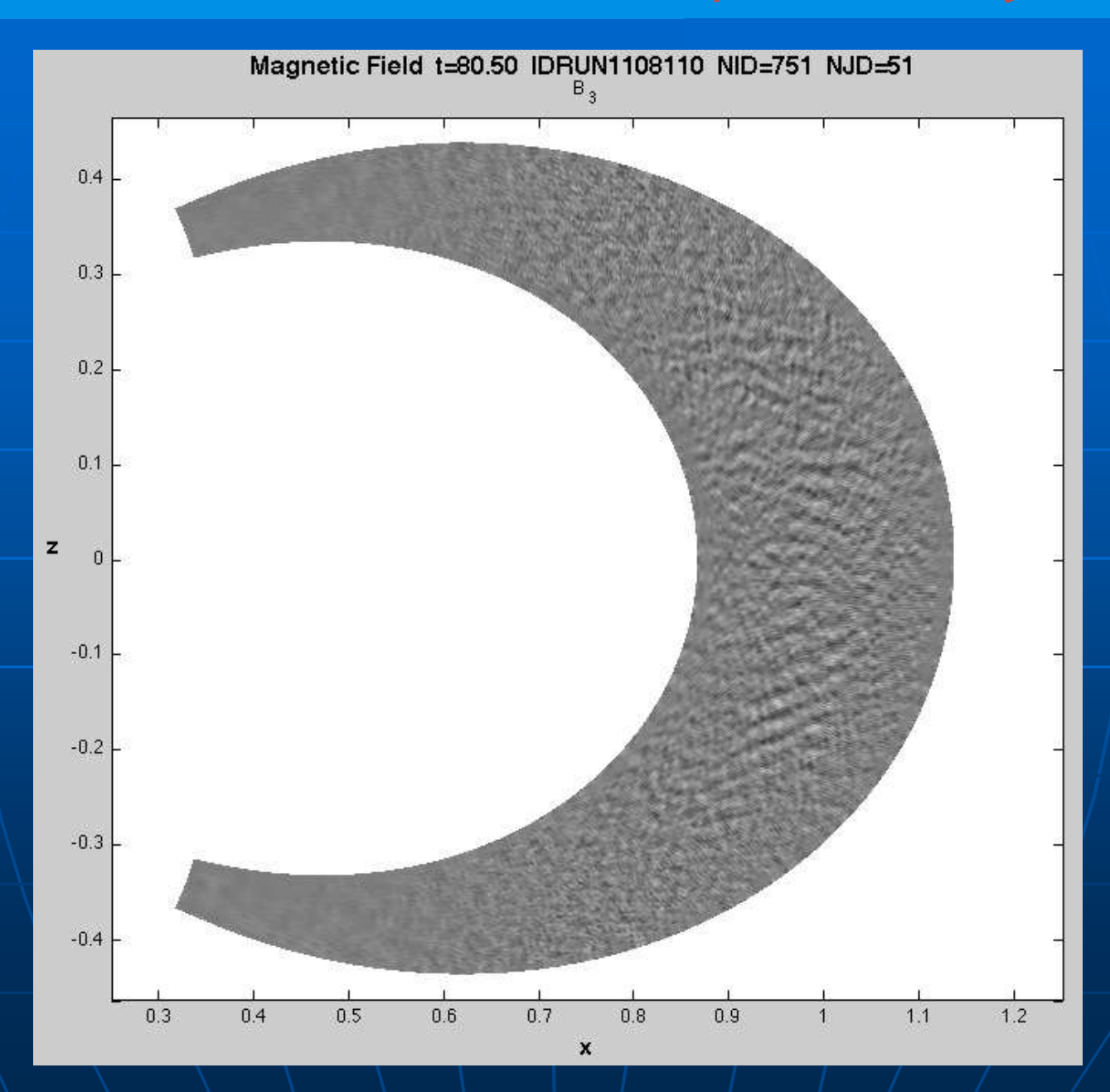
## Hybrid dipole simulations of whistler chorus due to $T_{perp}/T_{//} > 1$ , Wu and Denton

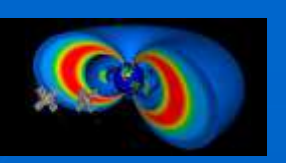
#### **Preliminary Results**

- Waves are generated near the equator and propagate away from to higher lattitude.
- Wave power peaks at the equator in a dipole field model.
- The chorus rising tone sweep rate is 60 times larger compared to observation due to assumed mag field inhomogeneity.

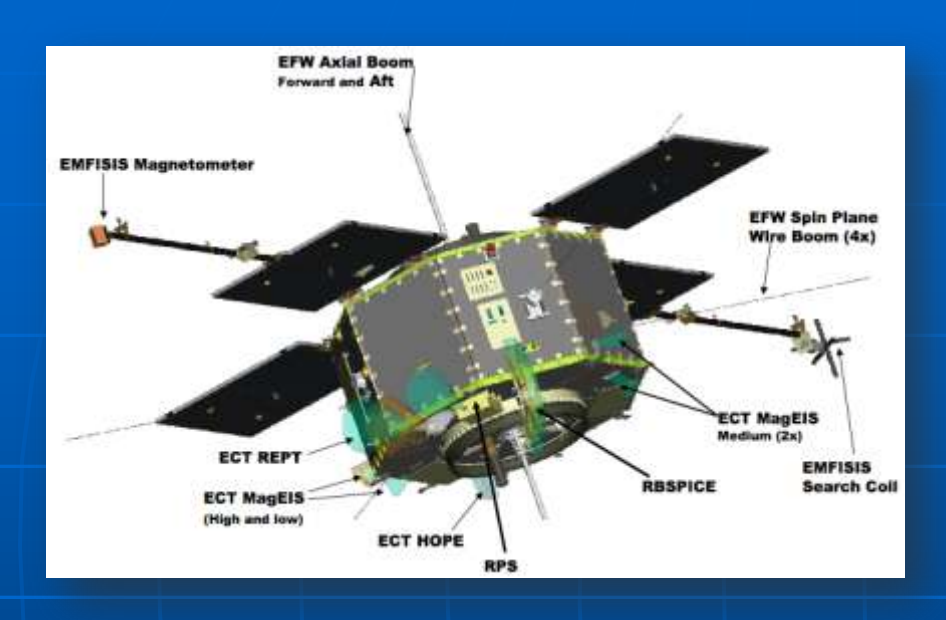


#### Hybrid Code Simulation – 2D preliminary results





#### Radiation Belt Storm Probes

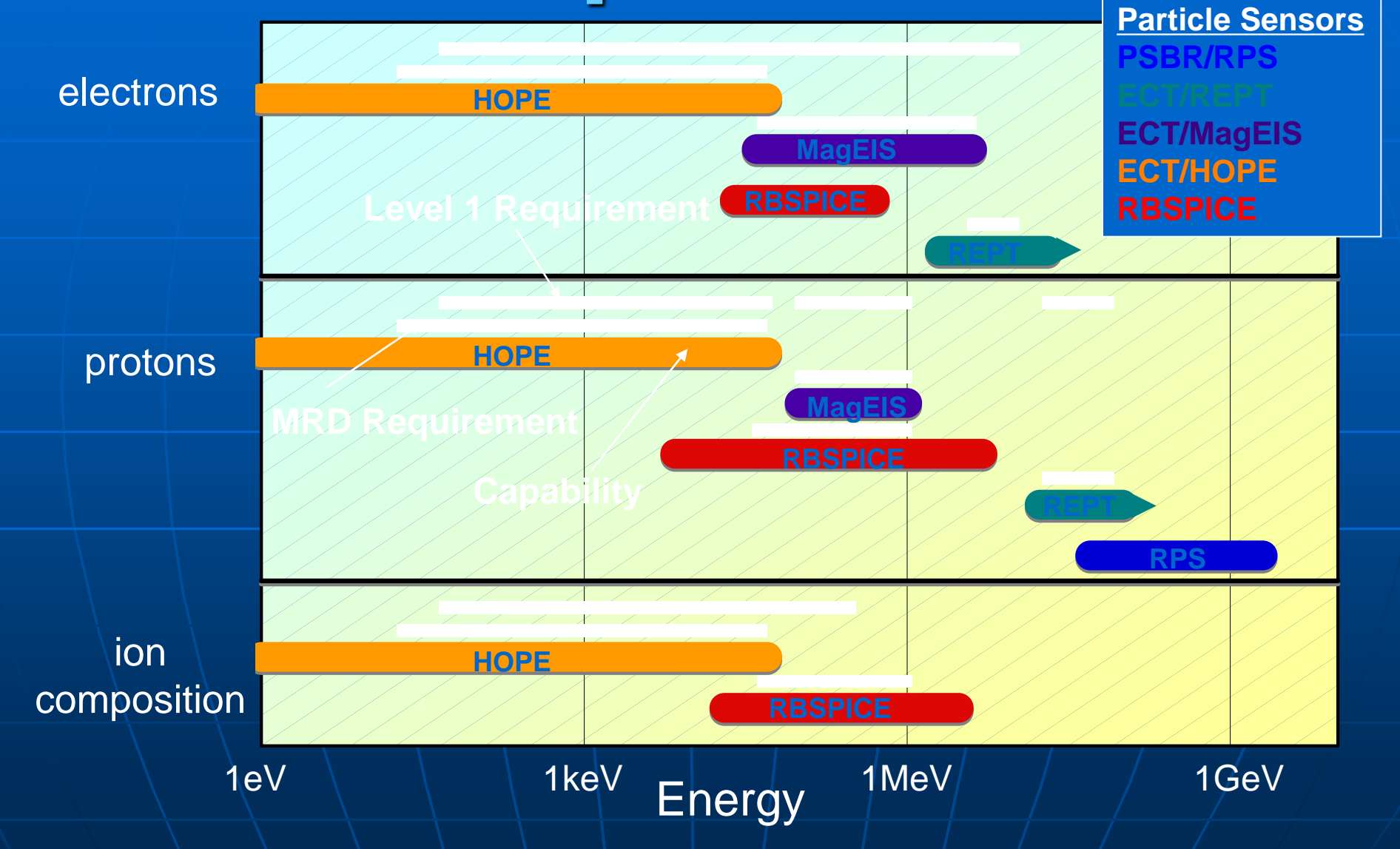




- Two identical highly-instrumented spacecraft, elliptical orbits (~600 km x 5.8 R<sub>F</sub>, 10° inclination)
- Expected launch August 23, 2012

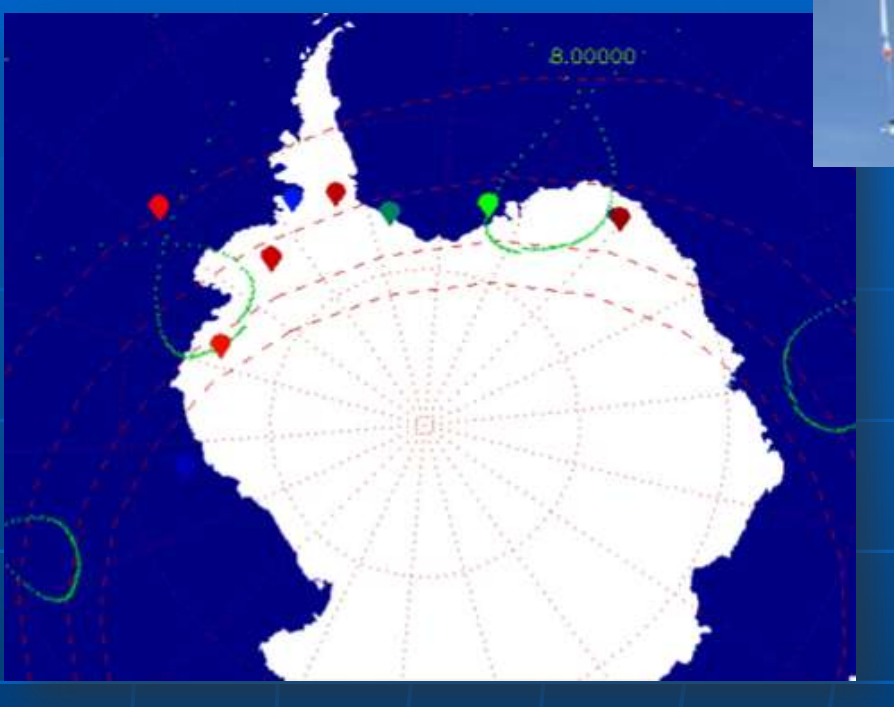


RBSP Particle Instrument Capabilities



## BARREL(Balloon Array for RBSP Relativistic Electron Losses)







Two campaigns - January 2013 and 2014

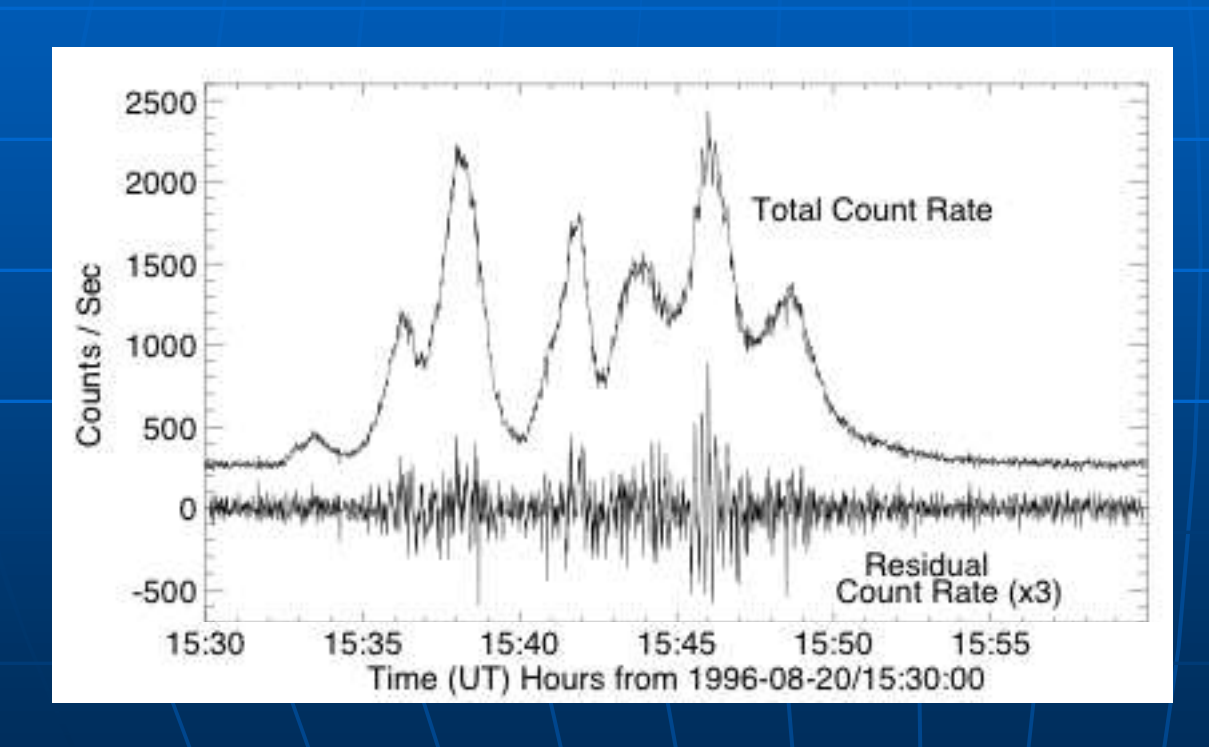
20 balloons launched each year

Make correlated measurements with RBSP



## BARREL Project: Precipitation Losses

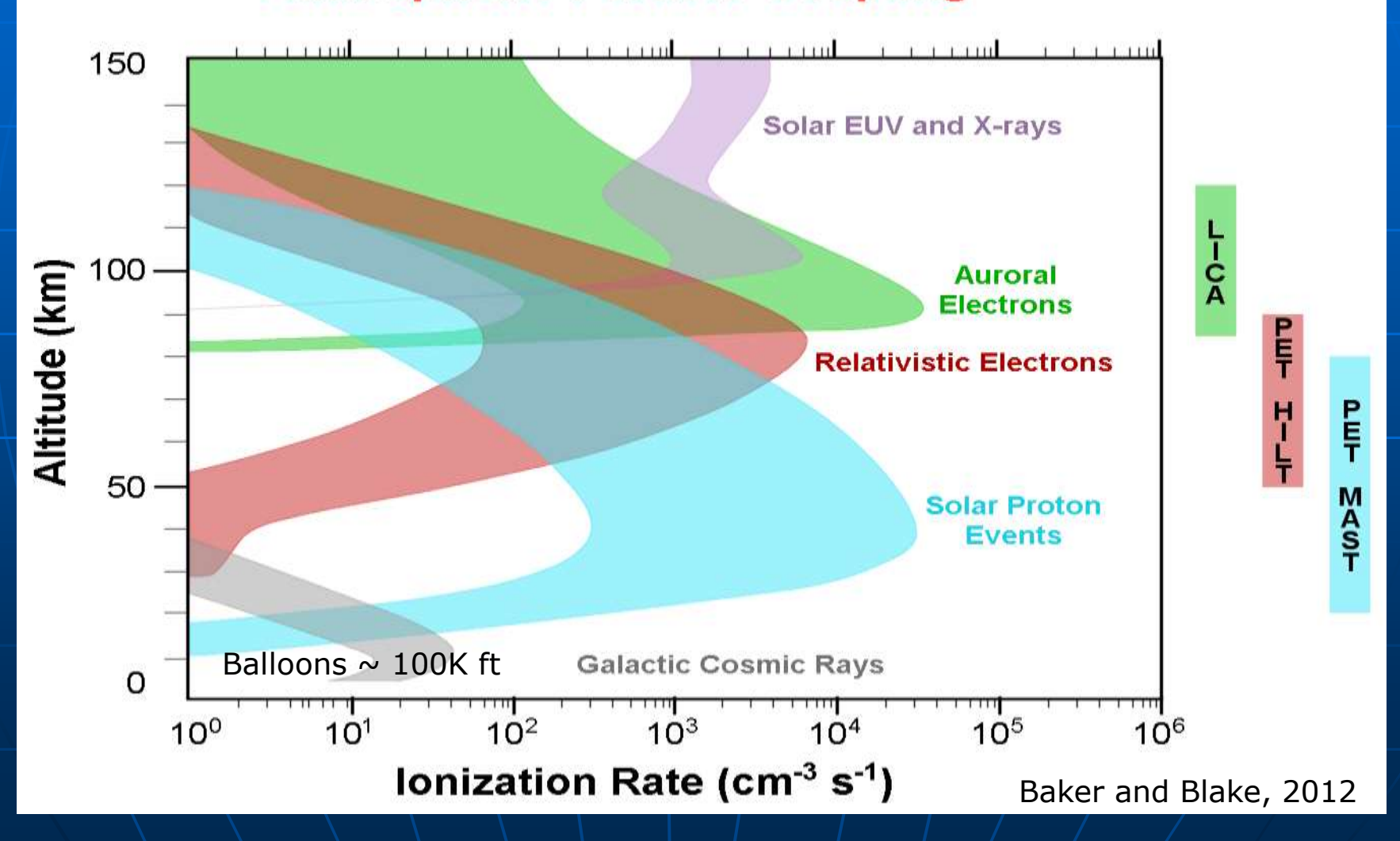
- Bremsstrahlung X-rays produced by precipitating electrons can be observed from stratospheric balloons
- Can separate spatial and temporal variations => complementary to spacecraft measurements





## Altitude of Energy Absorption

#### **Atmospheric Particle Coupling**



### Conclusions

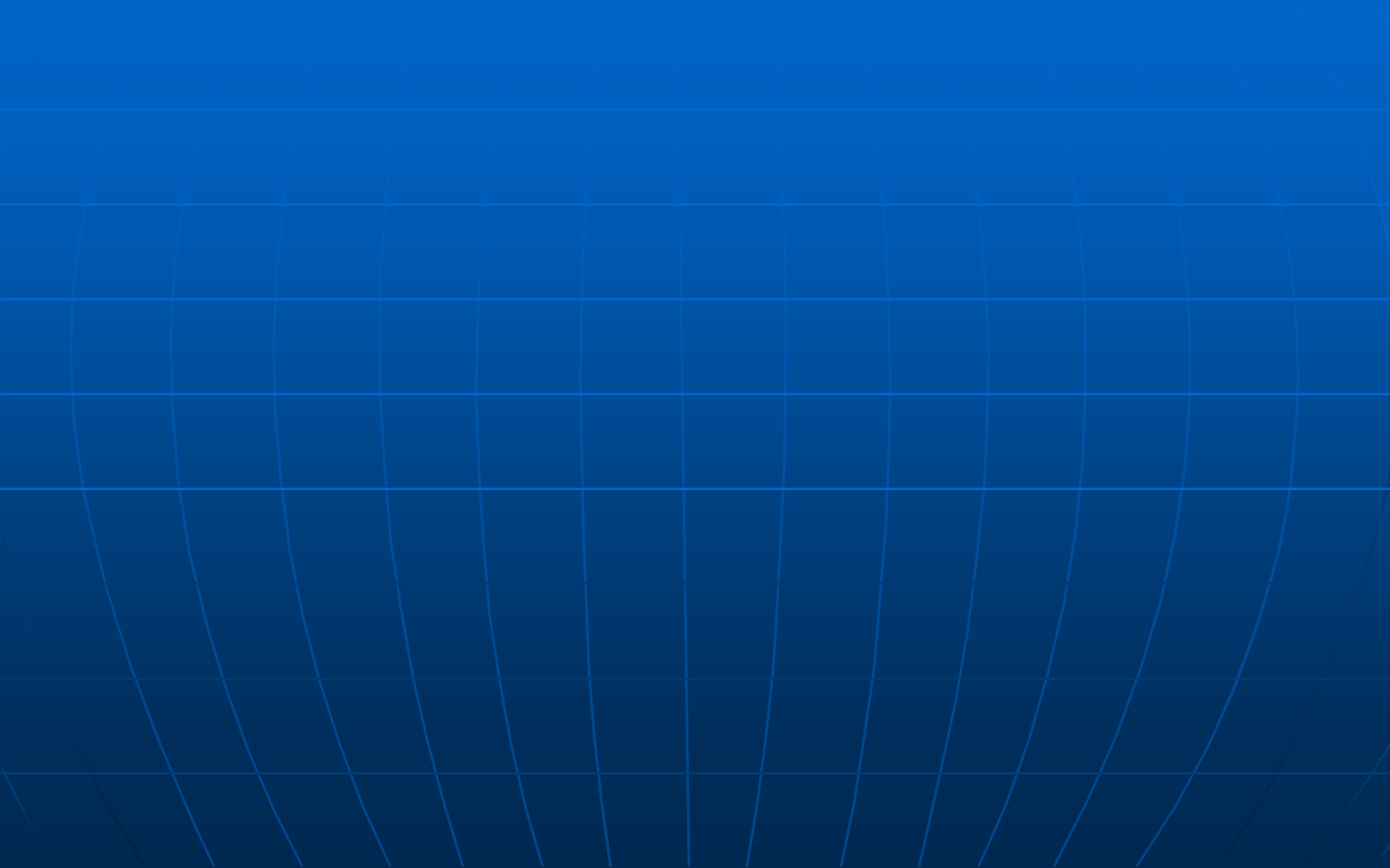
- Outer zone electrons have dynamic timehistory tied to solar variability
- Source and loss processes compete during active solar wind driving conditions
- Different time scales for outer zone variations
  - 1) Drift time scale (mins) injection of multi- MeV electrons:

Strong compression of dayside magnetopause due to high speed CME

## Conclusions cont.

- 2)Intermediate storm timescale (hrs,days):
  Changes described by convection, radial diffusion, loss to magnetopause (spatial);
  Localized heating balanced against loss due to whistler (and EMIC) scattering into atmosphere
- 3)Long time scales described by radial diffusion and pitch angle scattering losses to atmosphere D\_LL enhanced ~ 100x by ULF waves during active times; parametrized by Kp (B&A 2000) Causal link to solar cycle correlation with Vsw

## Extra Slides



## Source and Loss Balance

Over solar cycle, 276 Dst < -50 storms: 53% increase, 19% decrease, 28% same

